The Dead Forest of Chiefs Island: Soil Water Logging from Major Floods and Rainfalls Drive Rapid Vegetation Change in the Okavango Delta (Botswana)

Marc Jolivet, Mike Murray-Hudson, Kaelo Makati, Olivier Dauteuil, Louis Gaudare

Metadata of the article that will be visualized in OnlineFirst

ArticleTitle	The Dead Forest of Chiefs Island: Soil Water Logging from Major Floods and Rainfalls Drive Rapid Vegetation Change in the Okavango Delta (Botswana)	
Article Sub-Title		
Article CopyRight	The Author(s), under exclusive licence to Society of Wetland Scientists (This will be the copyright line in the final PDF)	
Journal Name	Wetlands	
Corresponding Author	FamilyName	**Jolivet**
	Particle	
	Given Name	**Marc**
	Suffix	
	Division	Géosciences Rennes, UMR-CNRS 6118
	Organization	University of Rennes
	Address	35042, Rennes, France
	Phone	
	Fax	
	Email	marc.jolivet@univ-rennes.fr
	URL	
	ORCID	http://orcid.org/0000-0002-1160-9386
Author	FamilyName	**Murray-Hudson**
	Particle	
	Given Name	**Mike**
	Suffix	
	Division	Okavango Research Institute
	Organization	University of Botswana
	Address	Private Bag 285, Maun, Botswana
	Phone	
	Fax	
	Email	
	URL	
	ORCID	
Author	FamilyName	**Makati**
	Particle	
	Given Name	**Kaelo**
	Suffix	
	Division	Okavango Research Institute
	Organization	University of Botswana
	Address	Private Bag 285, Maun, Botswana
	Phone	
	Fax	
	Email	
	URL	
	ORCID	
Author	FamilyName	**Dauteuil**
	Particle	
	Given Name	**Olivier**
	Suffix	
	Division	Géosciences Rennes, UMR-CNRS 6118

	Organization	University of Rennes
	Address	35042, Rennes, France
	Phone	
	Fax	
	Email	
	URL	
	ORCID	
Author	FamilyName	**Gaudare**
	Particle	
	Given Name	**Louis**
	Suffix	
	Division	Géosciences Rennes, UMR-CNRS 6118
	Organization	University of Rennes
	Address	35042, Rennes, France
	Phone	
	Fax	
	Email	
	URL	
	ORCID	

Schedule	Received	28 Aug 2023
	Revised	
	Accepted	8 Apr 2024

Abstract

The flood-controlled Okavango Delta in Botswana is an endoreic alluvial fan system developing within the arid to semi-arid Kalahari Desert. The Delta sustains a unique association of ecosystems, from rivers to floodplains, riverine forests to savanna forests. This complex environment is nearly pristine from anthropic activity but its preservation, especially in the face of global change, requires a detailed understanding of the functioning and evolution of its ecosystems. In this work we describe extensive tree dieback in the savanna forest of southern Chiefs Island, the largest permanently emerged island of the Delta. While tree dieback is generally linked to drought, extreme temperatures, fire or increased biotic attacks, we suggest that the destruction in the years 2009–2012 of the *Acacia* sp. and *Colophospernum mopane* dominated forest unexpectedly results from drowning through soil water logging associated to a series of successive exceptional floods and abundant rainfall seasons. This result highlights the necessity of transdisciplinary studies in understanding the autogenic functioning of the Delta as a prerequisite to describe the effects of global change.

Keywords (separated by '-') Forest dieback - Tropical Wetland - Flooding - Vegetation drowning - Southern Africa

Footnote Information The online version contains supplementary material available at https://doi.org/10.1007/s13157-024-01804-9 .

Wetlands _####################_
https://doi.org/10.1007/s13157-024-01804-9

ORIGINAL RESEARCH ARTICLE

The Dead Forest of Chiefs Island: Soil Water Logging from Major Floods and Rainfalls Drive Rapid Vegetation Change in the Okavango Delta (Botswana)

Marc Jolivet[1] · Mike Murray-Hudson[2] · Kaelo Makati[2] · Olivier Dauteuil[1] · Louis Gaudare[1]

Received: 28 August 2023 / Accepted: 8 April 2024

Abstract

The flood-controlled Okavango Delta in Botswana is an endoreic alluvial fan system developing within the arid to semi-arid Kalahari Desert. The Delta sustains a unique association of ecosystems, from rivers to floodplains, riverine forests to savanna forests. This complex environment is nearly pristine from anthropic activity but its preservation, especially in the face of global change, requires a detailed understanding of the functioning and evolution of its ecosystems. In this work we describe extensive tree dieback in the savanna forest of southern Chiefs Island, the largest permanently emerged island of the Delta. While tree dieback is generally linked to drought, extreme temperatures, fire or increased biotic attacks, we suggest that the destruction in the years 2009–2012 of the *Acacia* sp. and *Colophospermum mopane* dominated forest unexpectedly results from drowning through soil water logging associated to a series of successive exceptional floods and abundant rainfall seasons. This result highlights the necessity of transdisciplinary studies in understanding the autogenic functioning of the Delta as a prerequisite to describe the effects of global change.

Keywords Forest dieback · Tropical Wetland · Flooding · Vegetation drowning · Southern Africa

Introduction

The Okavango Delta in northern Botswana is an alluvial mega-fan deposited in the Okavango Graben, an active tectonic structure participating to the East African Rift System (McCarthy 2013; Pastier et al. 2017). The Delta represents a unique 18 000 km^2 sub-tropical wetland sustained by an annual flood bringing water from the highlands of Angola some 700 km to the North. This environment, enclosed within the Kalahari desert, makes for an exceptional biodiversity organized within several ecosystems (Ramberg et al. 2006; Mendelsohn et al. 2010) (Fig. 1). The Okavango alluvial fan can be separated in three main ecological compartments: permanent swamps, mostly to the North and East; seasonal floodplains in the central and southern parts; and drylands to the west and within the central part of many of the tens of thousands islands that emerge from the floodplains. This biological hot-spot faces the combined effects of global change and increasing anthropic pressure, and its preservation requires a detailed understanding of its ecological functioning. On the major islands emerging from the wetlands, the vegetation is dominated by savanna forests, a type of ecosystem known to be especially sensible to climate change (IPCC 2002). In general, forests are affected by global warming which triggered a worldwide increase in tree dieback, species migrations or population decrease (Jump et al. 2017; Pietrykowski and Woś 2021; Hartmann et al. 2022). Factors of tree mortality linked to climate change are mainly fire, drought, extreme temperature or increased biotic attacks favored by climate-induced physiological weakening of the plants (McGregor and O'Connor 2002; Hartmann et al. 2022). Some longer term mechanisms such as decreased seeding or complex interactions between fauna and flora are also leading to forest changes (Xu et al. 2019; Bush et al. 2020).

In this work we analyze the rapid decline – between 2006 and 2016 – of forest cover on Chiefs Island, the largest island (about 5 000 km^2) of the Okavango Delta. Indeed, while

✉ Marc Jolivet
marc.jolivet@univ-rennes.fr

[1] Géosciences Rennes, UMR-CNRS 6118, University of Rennes, 35042 Rennes, France

[2] Okavango Research Institute, University of Botswana, Private Bag 285, Maun, Botswana

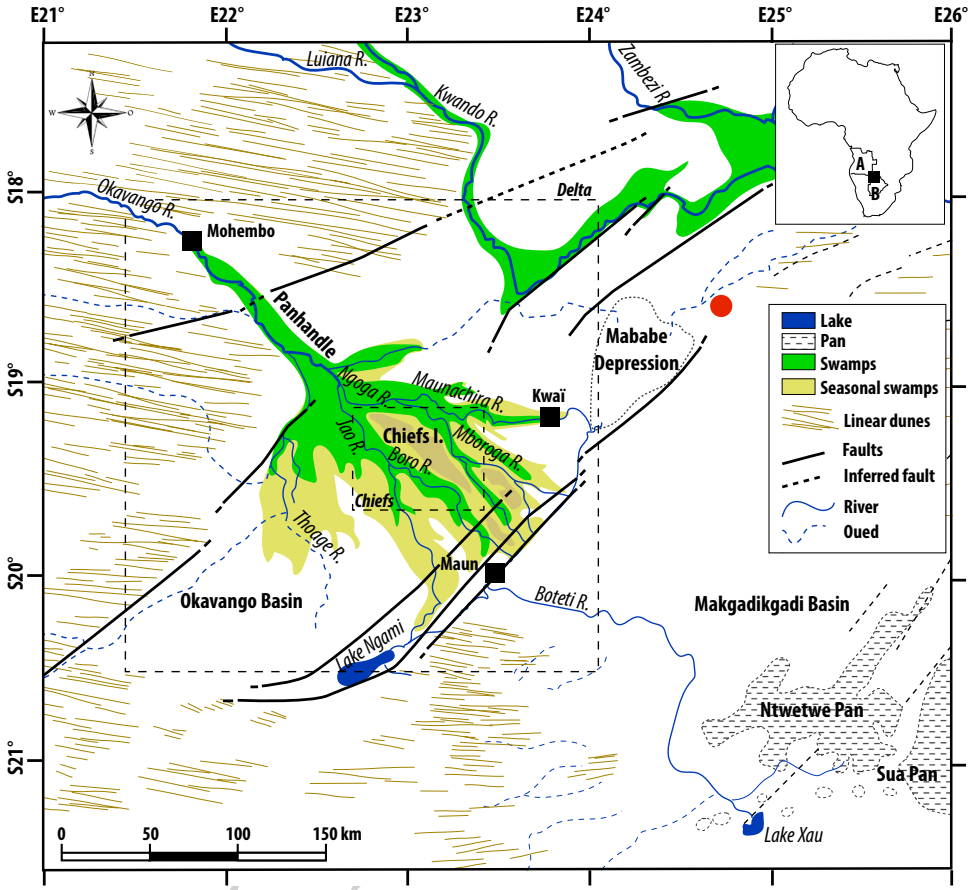

Fig. 1 Map of NW Botswana showing the Okavango Delta and the main locations discussed in the text. The areas represented in green correspond to permanently inundated regions while the seasonal swamps (in yellow) correspond to the major extension of the annual flood. The red dot indicates the location of the area of Fig. 4. Inset map of Africa: **A** Angola, **B** Botswana

pictures taken in the middle 1960th, show a dense savanna woodland covering most of the island (Fig. 2), the present-day landscape looks catastrophic, made of dead or barely surviving standing trees emerging from a tangle of large fallen trees (Fig. 2). The reasons for the destruction of that forest are unknown and the question remains whether it is a natural, although catastrophic evolution of the ecosystem or if there is a link with global change or regional anthropic activities.

Several products based on Landsat and Sentinel satellite images exist to follow the global evolution of forest or land cover. However very useful, these automatically generated classification maps are dedicated to some forest types (such as the European Tropical Forest Monitoring program (Vancutsen et al. 2021)) or lack the resolution to describe and monitor the evolution of complex environments such as the Okavango Delta (for example, the data provided by the University of Maryland Global Land Cover program (Hansen et al. 2022)) (Sup Fig. 1). In this study we thus rely on tree density measurements from high-resolution (< 1 m) satellite images, description of soil stratigraphy and geochemistry as well as flood and climate data analysis. We conclude that the Dead Forest of Chiefs Island largely results from drowning through soil water logging during an exceptional conjunction of major floods and high rainfalls in 2008—2011. We show that this event may have a strong influence on the ecological evolution of the area and shortly discuss its potential recurrence in the framework of the existing climate forecast models.

Environmental Setting of Chiefs Island

With a length of about 75 km and a maximal width of about 12 km, Chiefs Island is the largest island in the Okavango Delta (Figs. 1 and 3). Extending from S19.3° to S19.6 and E22.9 to E23.3, the island lies in the axial part of the Delta, and separates the alluvial fan into two compartments. To the West, the Thaoge, Jao and Boro channels show a contrasted flood season – dry season dynamics (Fig. 1). The permanently inundated area is restricted to the upper half of the river system, mainly along the Jao River while the Boro River is characterized by a seasonal floodplain that can occasionally become totally dry as in 2019. To the East, the Ngoga – Maunachira – Mboroga system is continuously inundated, the rivers only showing small seasonal changes (Gumbricht et al. 2004) (Fig. 1). The surface of Chiefs Island is characterized by a complex network of abandoned

Journal : Large 13157 | Article No : 1804 | Pages : 20 | MS Code : 1804 | Dispatch : 16-4-2024

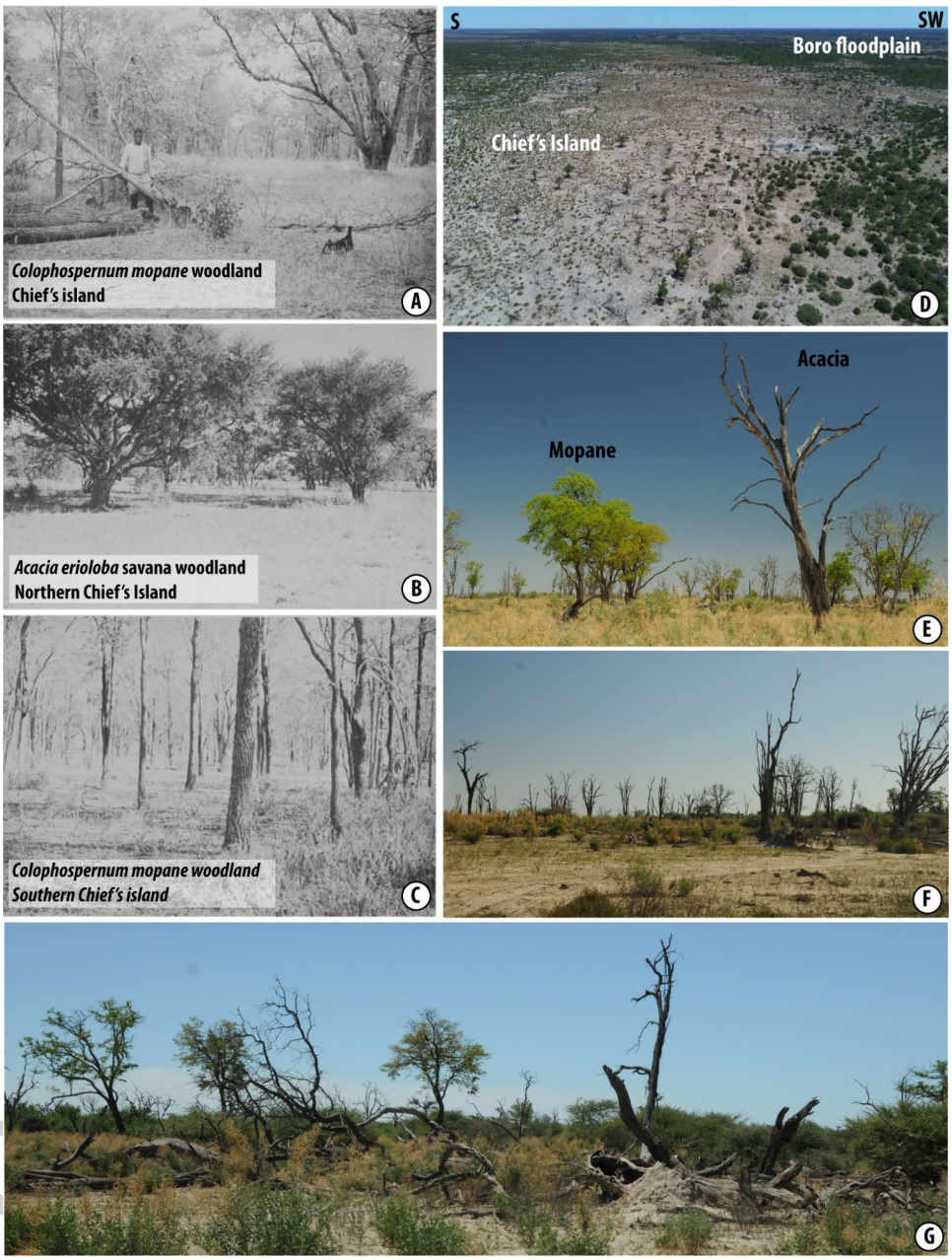

Fig. 2 Images of the vegetation on Chiefs Island. **A**, **B** and **C** Images taken in 1964 (from Biggs 1979) showing large *C. mopane* and *A. erioloba* trees in a savanna type forest. **D** Aerial picture of the SW edge of Chiefs Island showing the wide strip of dead trees (middle) separating the riverine forest developing along the edge of the island (right) from the "farmed mopanes" area (green area to the left). **E**, **F** and **G** Ground pictures showing the standing and fallen acacias and the surviving large mopanes (images M. Jolivet, November 2021)

paleo-channels, some of them several hundred meters wide. These paleo-structures are generally sandy (either white or reddish fine-grained sand) and support dryland types plant communities (Biggs 1979; Heath and Heath 2009). Although most of them are totally abandoned, some may still be flooded during strong or extreme flood events, sometimes leading to the death of the trees they support through drowning (Biggs 1979). Numerous ephemeral pools are also present, ranging in diameter from a few tens to several hundreds of meters. These are generally formed on clay-rich soils and devoid of vegetation. Like many islands in the Delta, the edges of Chiefs Island are characterized by a dense vegetation classified as riverine woodland or marginal vegetation (Biggs 1979; Ramberg et al. 2006a). This vegetation ring includes several species of large trees such as *Acacia nigrescens, Acacia erioloba*, *Philenoptera violacea* (rain tree), *Kigelia africana* (sausage tree) or *Combretum imberbe* (leadwood) as well as smaller bushes such as *Croton megalobotrys*. The vegetation inside the island is of savanna woodland type (as defined by Biggs 1979) or intermediate between woodland mixed and acacia scrub types (as defined by Heath and Heath 2009). Common species in that community are *Acacia hebeclada*, *Acacia erioloba* as well as bushes of *Pechuel-loeschea leubnitziae* (wild sage). Finally, large areas within the southern part of Chiefs Island are covered with *Colophospernum mopane* woodlands, some of them

Journal : Large 13157 | Article No : 1804 | Pages : 20 | MS Code : 1804 | Dispatch : 16-4-2024

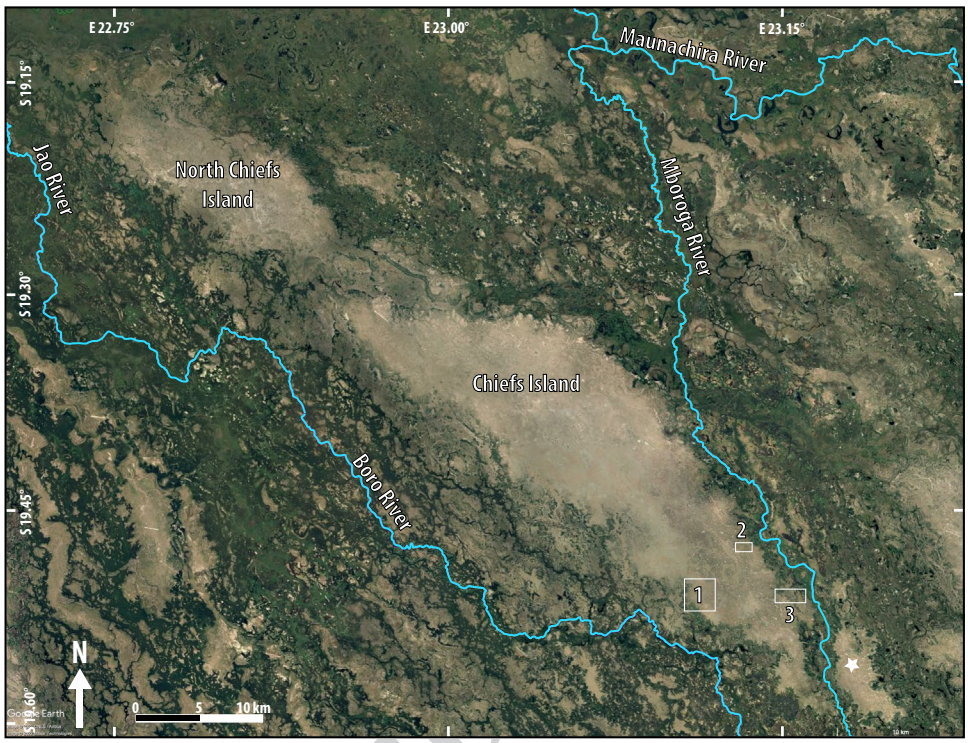

Fig. 3 Landsat (from Google Earth) satellite image showing Chiefs Island and the main channels as well as the location of the three zones in which trees have been counted (numbered white rectangles). The white star to the bottom right indicates the location of the pool discussed in the text and illustrated on Sup. Fig. 4

being strongly pruned by feeding elephants or other large herbivores such as buffalos (Smallie and O'Connor 2000) leading to the "farmed mopane" landscapes as described by Heath and Heath (2009). Few taller *C. mopane* specimens are preserved, associated to 5 to 15 m high dead acacias. Although Biggs (1979) indicated that mopane trees were restricted to the south-eastern part of the island, our field investigations in the Dead Forest on the western margin of the island showed 10 to possibly 20 m high mopane trees (of the "cathedral type described by Roodt 1992) indicative of soil conditions favorable to their growth (Sebego 1999; Makhado et al. 2014). In that area, mopanes are associated to 5 to 15 m high acacias (those are all dead) (Fig. 2). Given the growth rate of those two tree species, the c.a. 40 to 70 cm stem-diameter specimens forming the Dead Forest must be several tens of years old (possibly around 50 years) (Barnes et al. 1997; Cunningham and Detering 2017).

Data and Methods

Tree Density Analysis

High resolution satellite images available in Google Earth were used to map the variations in forest cover and in the distribution of the tree species, both on Chiefs Island and on key areas in the eastern part of the Okavango Delta. The most represented trees on Chiefs Island, *C. mopane* and acacias are deciduous, loosing their leaves during the driest season which may induce bias in the counting procedure, especially for small trees or in areas showing a high density of trees. In order to validate the approach, a 1 × 1 km quadrangle has been selected outside the Delta, in an area displaying both a savanna type forest and some open bushes – grassland vegetation (Figs. 1 and 4). The vegetation cover in that area appears stable through time except for the natural growth and death of trees. Two Google Earth satellite images were selected: i) July 2006, corresponding to the approximate timing of the first available image on Chiefs Island and showing trees with leaves and ii) September 2013 showing trees without leaves. For each image, trees and major bushes have been manually geo-referenced using the Google Earth application (Fig. 4). Using the QGIS software, geo-referenced trees were then superposed to a grid (19 × 19 cells of 54 × 55 m) and the number of trees in each grid was calculated to produce a tree-density map for both periods. The difference between the two density maps provides an estimation of the errors in distinguishing trees and estimating their number (Fig. 4). Overall, the difference in counts is 7% (111 points) and counting performed during the dry season (no leaves) shows a higher number (1691 instead of 1580). When trees have leaves, some of the canopies – especially for the smallest trees and bushes – are merged while trunks are easier to distinguish in the absence of leaves. Alternatively, small bushes, especially in the open bushes-grassland areas are harder to spot when free of leaves. The final error on tree counting may be reduced by comparing several images and spotting "missing" points.

Journal : Large 13157 | Article No : 1804 | Pages : 20 | MS Code : 1804 | Dispatch : 16-4-2024

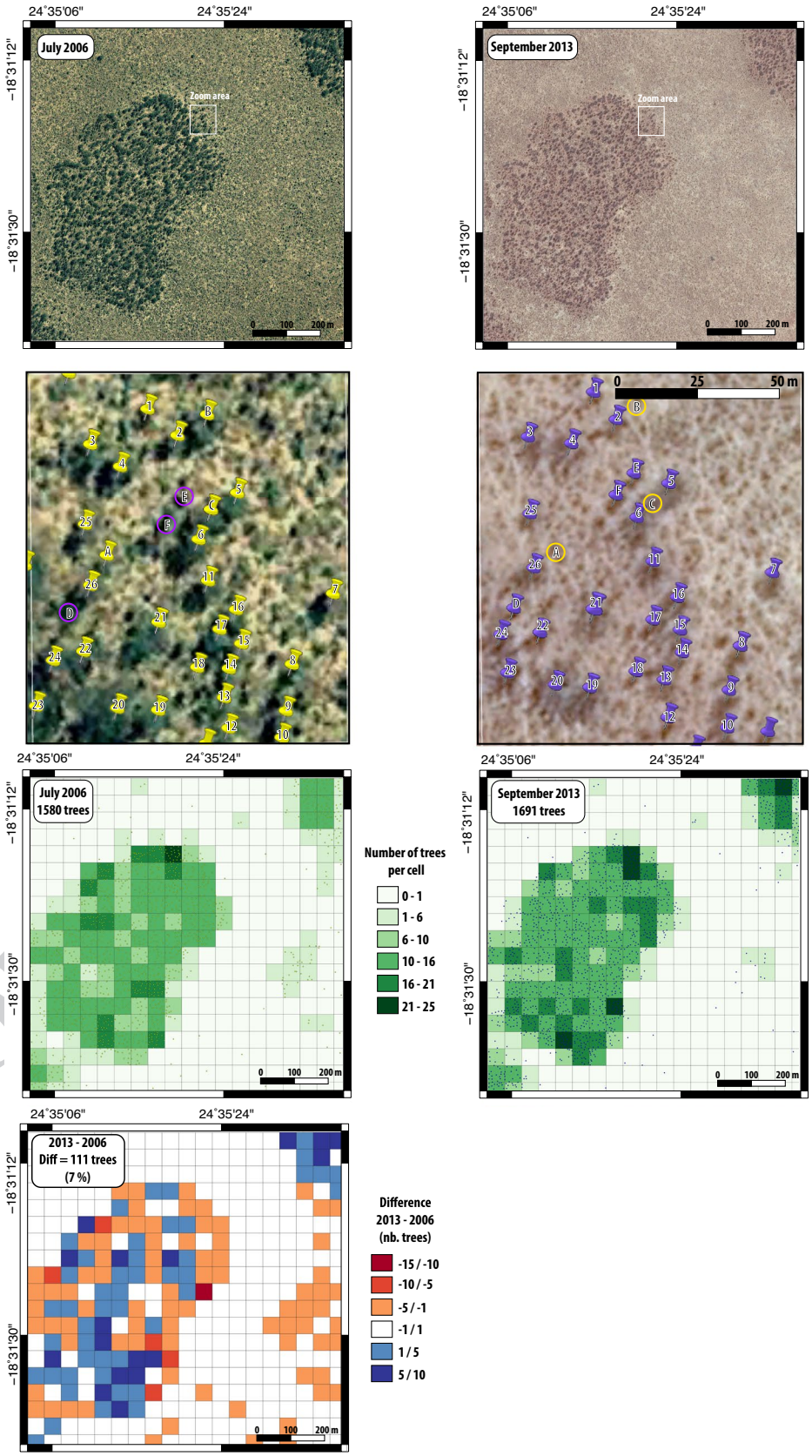

Fig. 4 Approach validation. Mixed savanna-forest and bushes-grassland area selected to test the tree-counting approach (see location on Fig. 1). Two images have been selected, one showing trees with leaves (July 2006) and the second showing bare trees (September 2013). The two zoomed images show pins referencing the location of each trees. Pins with numbers indicate corresponding trees on each picture while pins with letters refer to trees that are missing on one or the other picture (purple and orange circles). The graphs with green cells represent tree density maps derived from the above counting. The number of trees counted during the dry season (no leaves) is higher by 7% than the number of trees counted during the wet season (leaves). The bottom graph is the difference between the 2013 and 2006 density maps. The difference in counting is mostly due to the fact that individual trunks are easier to distinguish than merged canopies (see blue cells on bottom graph). However, small bushes, especially in the open grassland area and along the edges of the savanna forest area are easier to spot when having leaves (see red and orange cells on bottom graph)

Journal : Large 13157 | Article No : 1804 | Pages : 20 | MS Code : 1804 | Dispatch : 16-4-2024

Based on the results obtained on the test area, manually counting trees on high resolution images can thus be considered as a valid approach to quantify the evolution of savanna-type forest cover. Seasonality, although inducing errors when dealing with deciduous trees is not a major pitfall. The error margin on counting is of the order of 5 to 10% depending on the size of the trees and their density. Indeed, the approach is limited by the capacity to separate the individual tree canopies and could not be applied in dense forests.

To estimate the variation in tree-cover density on Chiefs Island, we selected three representative areas on the southern part of the island where good-resolution (trees can be individualized) satellite images were available over the period 2006 – 2018 (Fig. 3). Zone 1 is a 3.56 km^2 rectangle situated on the western side of the island and including both the tree ring along the Boro River floodplain and the central part of the island. Zone 2 is a 2 km^2 rectangle on the eastern part of the island, largely inside the central zone, crossed by a N-S sometimes-flooded channel in its axial part. Finally Zone 3 is a 0.86 km^2 rectangle situated to the east of the island in the central zone. The position of individual trees in Zone 1 was determined on 5 images (2006, 2011, 2012, 2016, 2018) in order to obtain the most complete evolution of the tree population. Zones 2 and 3 were only investigated for years 2006 and 2016 for comparison. Most of the satellite images available on Google Earth were taken during late austral summer to autumn when trees have leaves. Only the 2018 image, taken in November shows bare trees (Fig. 5). By comparing with field pictures taken in November 2021 (Fig. 2) and showing large mopanes with few leaves and standing acacia trunks, we decided to include in our counting all standing trees showing branches. This probably maximizes the number of living trees. Each zone was then superposed to a grid (19 × 17 cells of 104 × 104 m for Zone 1; 24 × 7 cells of 105 × 105 m for Zone 2; 11 × 6 cells of 94 × 130 m for Zone 3) and the number of trees in each grid was calculated to produce tree-density maps (Fig. 6 and Sup. Fig. 2). Finally, major surface features such as zones covered with small bushes, pools or occasionally active channels (Zone 2) have been mapped from Google Earth images to be superposed to tree mapping (Fig. 5 and Sup. Fig. 3).

Soil Description and Major Elements Geochemistry

The soil structure, its lithology and its chemical composition also play a major role in the development of the vegetation. The occurrence of salt (mainly natronite) has long been documented on islands of the Okavango Delta (McCarthy et al. 1986), and a sudden rise in the alkalinity of the soil may have an impact of the vegetation. Soil structure and lithology (through permeability and porosity) control groundwater infiltration, both horizontally (infiltration of flood water) and vertically (infiltration of rain water and rise of the water table) (Ramberg et al. 2006b; Wolski and Savenije 2006).

Some studies have investigated the soil stratigraphy and hydraulic properties in a few islands of the Delta (McCarthy et al. 1991; McCarthy and Ellery 1994; Wolski and Savenije 2006). Detailed sedimentary logs are seldom published (Jolivet et al. 2023, 2024) and to our knowledge none are available on Chiefs Island. Similarly, no soil geochemistry data are available, especially to document the potential occurrence of salt. Finally, aside for some large-scale models, based on remote sensing analysis (Milzow et al. 2009), the depth of the water as never been measured and remains unknown.

In this study we investigated the lithology and stratigraphy of the soil in Chiefs Island through manual auger drilling in three key areas of Zone 1 (Fig. 5). Samples were collected about every 20 to 30 cm in each hole to build a stratigraphic log (Fig. 7). The two first drill holes (DH-1 and DH-2) were made in November 2021 at the beginning of the rain season while DH-3 was done in July 2022 during the dry season. Drill hole 1 (DH-1: S19.501790°/E23.181200°, depth of 3 m) was situated close to the tree line bordering Chiefs Island to the West, in a sandy area slightly higher than the surroundings and mainly covered with wild sage and grass. DH-2 (S19.501693°/E23.181999°, depth of 7 m) was located further inside the island, some 80 m from DH-1 in a small depression showing an apparently more clay- (the amount of clay is estimated visually in the field from the cohesive behavior of the wet sediment) and organic matter-rich (the amount of organic matter (OM) is evaluated visually from the color of the sediment) surface soil. Vegetation was scarce, mainly represented by *Orthanthera jasminiflora* and few grasses. The limit between the sandy area and the depression was marked by bushes of *C. Megalobotris* and acacias. No water was observed on the surface in the central part of that depression at the time of drilling but the ground had been plowed by elephants suggesting ephemeral occurrence of water during the rainy season (although none of the high-resolution satellite images available on Google Earth shows water). DH-3 (S19.505678°/E23.188336°, depth of 6 m), located further inside the island, was drilled on the edge of a large pool containing water at the time of drilling. The soil outside the pool area was sandy and over a wide area surrounding the pool, vegetation was composed of small "farmed type" mopanes pruned by elephants, some grasses and few wild sage bushes. Inside the pool area, the surface soil was again clay- and OM-rich and vegetation was only represented, on the less frequently flooded edge, by *Orthanthera jasminiflora*.

The major elements geochemistry of soil samples collected along profiles DH-1 and DH-2 was analyzed especially in order to detect a potential anomalous concentration of salt (NaCl and KCl) that could explain the tree mortality. The carbonate concentration was also

Journal : Large 13157 | Article No : 1804 | Pages : 20 | MS Code : 1804 | Dispatch : 16-4-2024

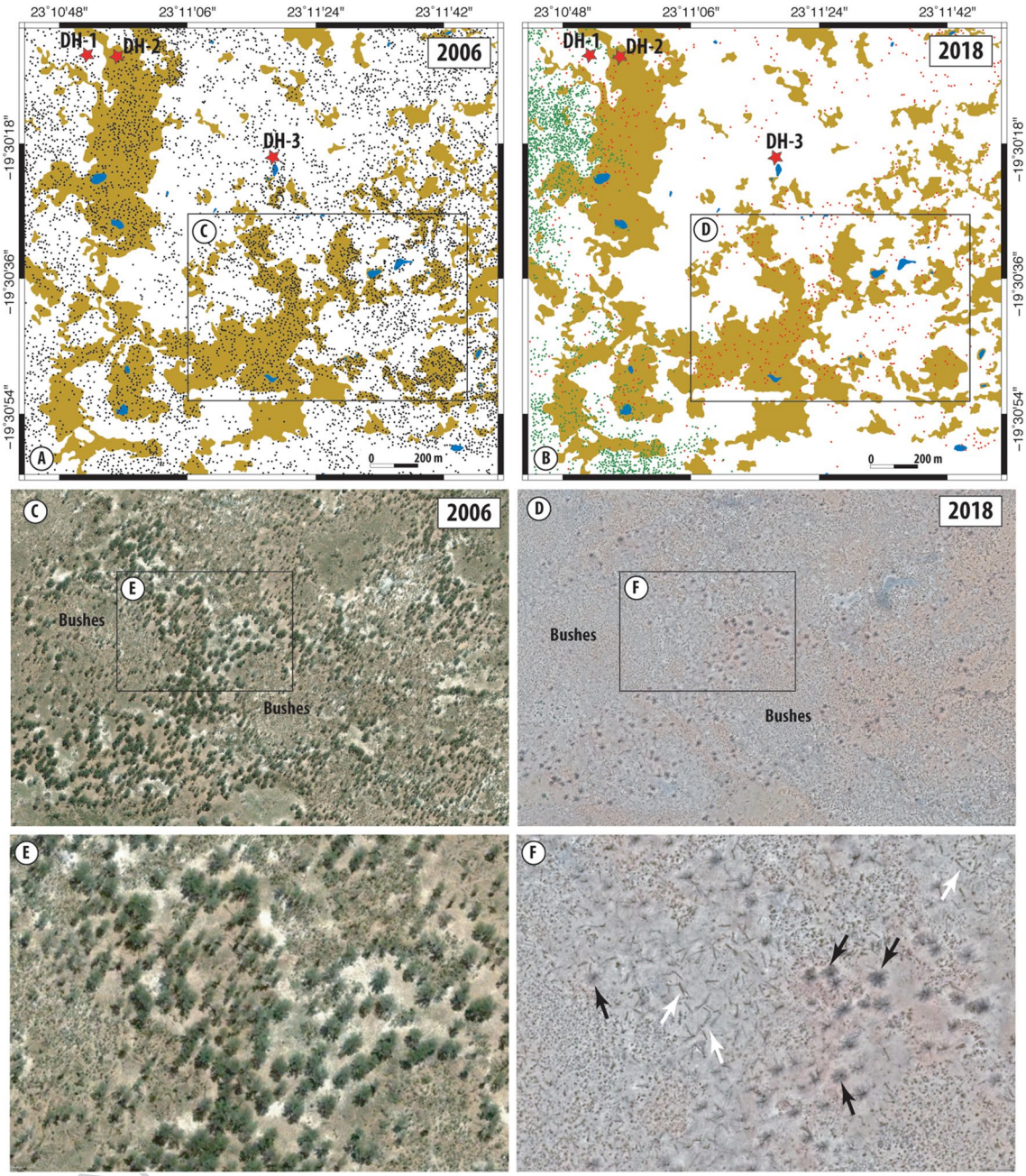

Fig. 5 **A** and **B** Physiographic map of Zone-1 showing the distribution of the standing trees in 2006 (**A**) and 2018 (**B**). On Fig. 5A, the black dots represent all the living trees. On Fig. 4B, the green dots correspond to living trees on the outer vegetation ring, the red dots correspond to the standing, leafless trees within the central part. The red starts indicate the position of the drill holes. The brown areas are the regions corresponding to slight depressions without bushes. The blue areas are the pools containing water in 2018. **C** and **D** two images of the vegetation in 2006 and 2018 (with zooms on images **E** and **F**) showing the near complete destruction of the forest. Note the fallen trees (white arrows) and the still standing but leafless trees (black arrows) on image F

measured as a good indicator of root activity: CO_2 respiration induces the production of carbonic acid that hydrolyzes minerals in the area of the ground were root activity occurs. This reaction is rapidly neutralized below the root layer and carbonate precipitates, generally as nodules (Retallack 2005). After being reduced to powder, samples were analyzed at the French national Service d'Analyse des Roches et Minéraux (SARM) in Nancy using an ICP-EOS iCap6500 spectrometer. Data are summarized in Table 1.

Journal : Large 13157 | Article No : 1804 | Pages : 20 | MS Code : 1804 | Dispatch : 16-4-2024

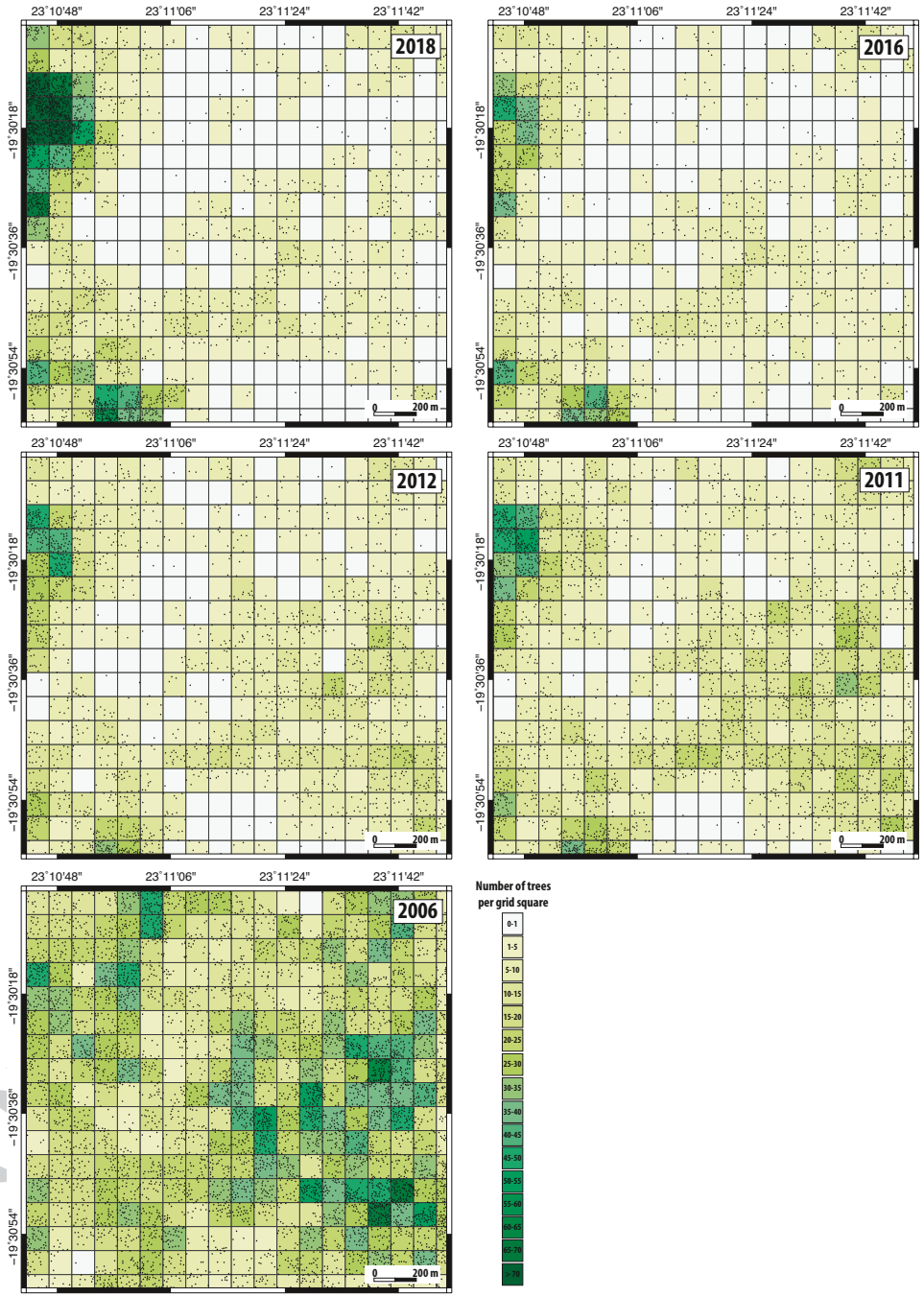

Fig. 6 Map of the density of trees on Zone-1 in 2006, 2011, 2012, 2016 and 2018. See text for discussion and Fig. 3 for the location of Zone-1. The intensity of the green color indicates the number of trees per counting cell. Black dots indicate the individual trees

Hydrology

Medium-resolution (10 to 30 m pixels) satellite images such as Landsat or Sentinel products are valuable tools to follow the dynamics of floods in wetlands, although only the open-water bodies (drains, pools, lakes) and, to some extend the low-vegetation floodplains can be reasonably monitored (monitoring the flood propagation in dense, high reeds or papyrus vegetation remains a challenge). Unfortunately no Landsat images are available for the Okavango Delta for the years 2008 to 2012 and the Sentinel-1 radar satellite was launched in 2014. As a proxy to the intensity of the flood, water discharge data from the Mohembo station situated at the entry of the Panhandle (Fig. 1) were obtained from the Okavango Research Institute online catalog (http://www.okavangodata.ub.bw/ori/). Water discharge at the inlet of the Delta does not directly determine the extent of the downstream flooding as the propagation of the flood depends on the intensity of the previous-year flood and rainfalls. Indeed,

Journal : Large 13157 | Article No : 1804 | Pages : 20 | MS Code : 1804 | Dispatch : 16-4-2024

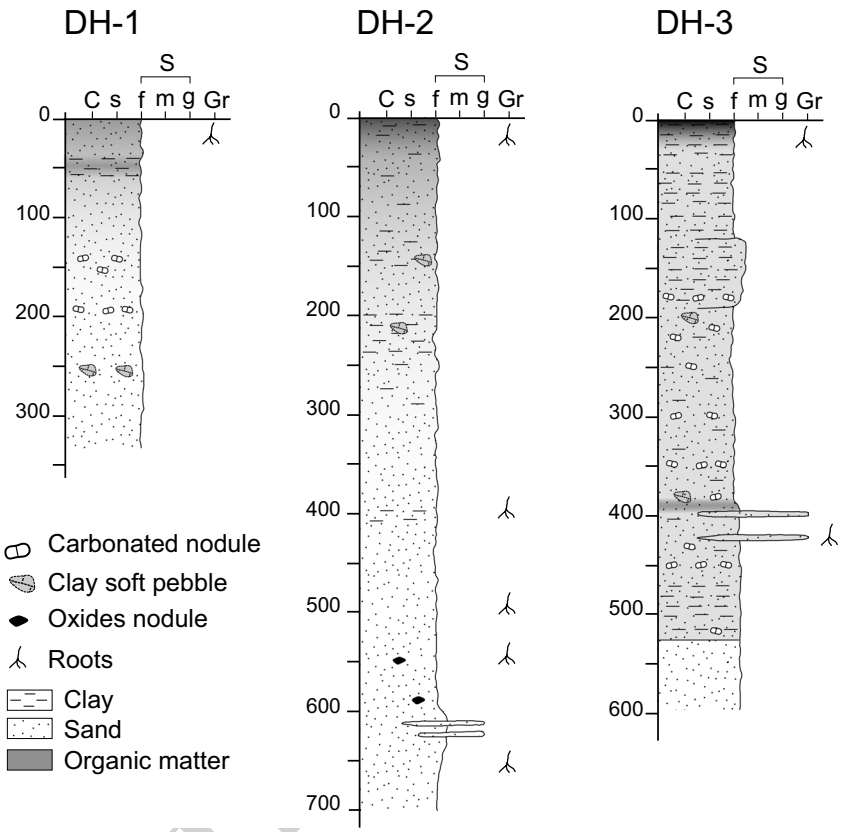

Fig. 7 Sedimentary log of the three drill holes made in Zone-1. Note the absence of carbonated nodules in DH-2 and the very sharp transition at 530 cm in DH-3 between OM- and clay-bearing sediment and clear, white sand. See text for a complete description

a large volume of the flood-water infiltrates, refilling the groundwater aquifer and only when the ground water table reaches the surface does the surface flood propagate farther (Gumbricht et al. 2004; Milzow et al. 2009). However, the long-term evolution of water discharge at Mohembo gives a first order information on the long-term flood extent pattern. Daily measurements cover the period from December 1974 to Mai 2022 but there are gaps in the data from February 2010. Those gaps were "filled" using linear regression between two adjacent points minimizing the errors, although maximums and minimums in the discharge pattern may be minimized and maximized, respectively (Fig. 8).

Monthly rainfall measurements from 1970 to 2012 at Maun airport (Figs. 1 and 9) were also obtained from the Okavango Research Institute online catalog. Although Maun is situated some 70 km to the South from the centre of Chiefs Island and some local variations in precipitation can be expected, this direct record is the nearest and most complete available. Rainfall values from CHIRPS data (Funk et al. 2014, 2015) were used to complete the Maun airport rainfall data and provide a larger-scale precipitation model for the Delta and Chiefs Island regions over the period 1981 – 2020 (see the extend of the selected zones for Chiefs Island and the Delta on Fig. 1). For comparison with the measured data, the precipitation data from the CHIRPS pixel corresponding to Maun airport were also extracted.

Based on daily records in Maun airport and the CHIRPS data, annual rainfalls time-series have been calculated over a calendar basis (January to December) as well as total rainfall during the rainy season (Fig. 9). The duration of the latest (generally covering the period from September to May with some variations) has been calculated for each year considering that it corresponds to 3 or more consecutive months with more than 3 mm of rain.

Results

Tree Density Analysis

Zone 1

A total of 7166 trees have been counted in Zone 1 for 2006 (Table 2). Based on observation of the satellite image, trees were mostly present in sandy low areas including the water pools and devoid of wild sage bushes. However, some of those low areas probably corresponding to paleo-channels, remain barren (down to tree densities of 0 per counting cell), only covered with grass. The maximum density of trees (69 per counting cell (cc)) was obtained in the SE quadrangle

Table 1 Major elements geochemistry of soil samples from drill holes 1 and 2

Sample name	SiO2 %	Al2O3 %	Fe2O3 %	MnO %	MgO %	CaO %	Na2O %	K2O %	TiO2 %	P2O5 %	LOI %	Total %
Detection limit	0.05	0.04	0.015	0.015	0.03	0.03	0.02	0.03	0.02	0.10		
DH-1 / 0	96.64	1.227	0.328	< L.D.	0.074	0.075	0.025	0.204	0.084	< L.D.	1.75	100.4
DH-1 / 30	95.93	1.56	0.407	< L.D.	0.09	0.098	0.028	0.248	0.104	< L.D.	1.69	100.2
DH-1 / 60	96.55	2.228	0.607	< L.D.	0.142	0.121	0.027	0.255	0.115	< L.D.	1.88	100.9
DH-1 / 122	95.36	2.17	0.6	< L.D.	0.151	0.141	0.025	0.255	0.106	< L.D.	2.18	101
DH-1 / 150	92.71	2.6	0.74	< L.D.	0.219	0.365	0.029	0.298	0.129	< L.D.	2.9	100
DH-1 / 184	88.98	2.199	0.624	< L.D.	0.305	2.862	< L.D.	0.292	0.114	< L.D.	4.28	99.7
DH-1 / 226	96.42	0.73	0.194	< L.D.	0.074	0.528	< L.D.	0.157	0.057	< L.D.	0.96	99.1
DH-1 / 250	97.4	0.41	0.104	< L.D.	0.032	0.221	< L.D.	0.118	0.043	< L.D.	0.65	99
DH-1 / 280	96.18	0.446	0.112	< L.D.	0.041	0.315	< L.D.	0.121	0.043	< L.D.	0.74	100
DH-1 / 318	96.69	0.462	0.118	< L.D.	0.035	0.198	< L.D.	0.112	0.038	< L.D.	0.6	100.2
DH-2 / 10	96.84	0.984	0.221	< L.D.	0.036	0.044	< L.D.	0.161	0.078	< L.D.	1.08	99.5
DH-2 / 50	96.95	0.882	0.187	< L.D.	< L.D.	0.03	< L.D.	0.196	0.088	< L.D.	0.82	99.2
DH-2 / 120	97.83	0.588	0.111	< L.D.	< L.D.	< L.D.	< L.D.	0.15	0.06	< L.D.	0.49	99.2
DH-2 / 150	97.92	0.784	0.159	< L.D.	< L.D.	< L.D.	0.025	0.214	0.101	< L.D.	0.85	100
DH-2 / 220	96.53	1.095	0.221	< L.D.	0.032	0.031	0.025	0.247	0.125	< L.D.	0.68	101
DH-2 / 250	96.38	1.072	0.228	< L.D.	0.038	0.038	0.02	0.209	0.091	< L.D.	0.69	100.8
DH-2 / 310	97.78	0.808	0.161	< L.D.	< L.D.	< L.D.	< L.D.	0.168	0.069	< L.D.	0.48	99.5
DH-2 / 350	97.6	0.585	0.105	< L.D.	< L.D.	< L.D.	0.023	0.212	0.091	< L.D.	0.38	99.
DH-2 / 410	97.89	0.607	0.101	< L.D.	< L.D.	< L.D.	< L.D.	0.111	0.048	< L.D.	0.61	99.8
DH-2 / 450	97.74	0.326	0.065	< L.D.	< L.D.	< L.D.	< L.D.	0.07	0.035	< L.D.	0.75	99.
DH-2 / 510	98.65	0.5	0.104	< L.D.	< L.D.	< L.D.	< L.D.	0.108	0.048	< L.D.	0.11	99.7
DH-2 / 570	98.38	0.332	0.071	< L.D.	< L.D.	< L.D.	< L.D.	0.066	0.031	< L.D.	0.18	99
DH-2 / 600	98.4	0.3	0.055	< L.D.	< L.D.	< L.D.	< L.D.	0.087	0.023	< L.D.	0.17	99
DH-2 / 660	99.24	0.414	0.085	< L.D.	< L.D.	< L.D.	< L.D.	0.137	0.068	< L.D.	0.27	100.2
DH-2 / 700	97.75	0.37	0.072	< L.D.	< L.D.	< L.D.	< L.D.	0.114	0.051	< L.D.	0.42	98.8

The number following the / in the sample names indicate the sampling depth in cm. < L.D. indicates values below detection limits. *LOI* Loss on ignition

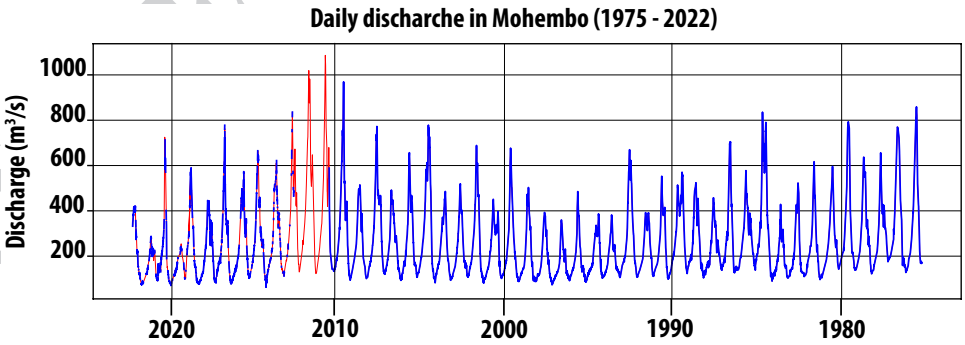

Fig. 8 **A** Daily discharge at Mohembo from 1975 to 2022, measured (blue) and interpolated from uncomplete measurement data (red). See text for interpolation method

of Zone 1 which generally showed a higher mean density than the rest of the area (Figs. 6 and 10). To the West, the external tree-ring separating the island from the Boro River floodplain was difficult to distinguish from the rest of the tree-cover, with a maximum tree density of 50 per cc. A number of fallen tree trunks were visible in several of the forested areas, but generally in a limited amount that could correspond to the background mortality, although no information exists on this.

In 2011, the total number of counted trees was 3064, representing a 57% loss compared to 2006 (Table 2). The formerly highly forested SE quadrangle displayed a major loss, only reaching a maximum tree density of 30 to 35 per cc (Figs. 6 and 10). On the contrary, the tree density in the outer ring did not decrease, still reaching a maximum of 51 per cc.

In 2012, the total tree number falls down to 2293 (loss of 68% compared to 2006) (Table 2). The maximum density in the SE quadrangle was 20 to 25 trees per cc while most of the area situated east of the western outer tree ring was barren (Fig. 6). In the latest, the tree density remained stable or decreased only very slightly with a maximum between 45 and 50 per cc. However, from the images, most of the large trees in that ring had also fallen, replaced by small bushes of

Journal : Large 13157 | Article No : 1804 | Pages : 20 | MS Code : 1804 | Dispatch : 16-4-2024

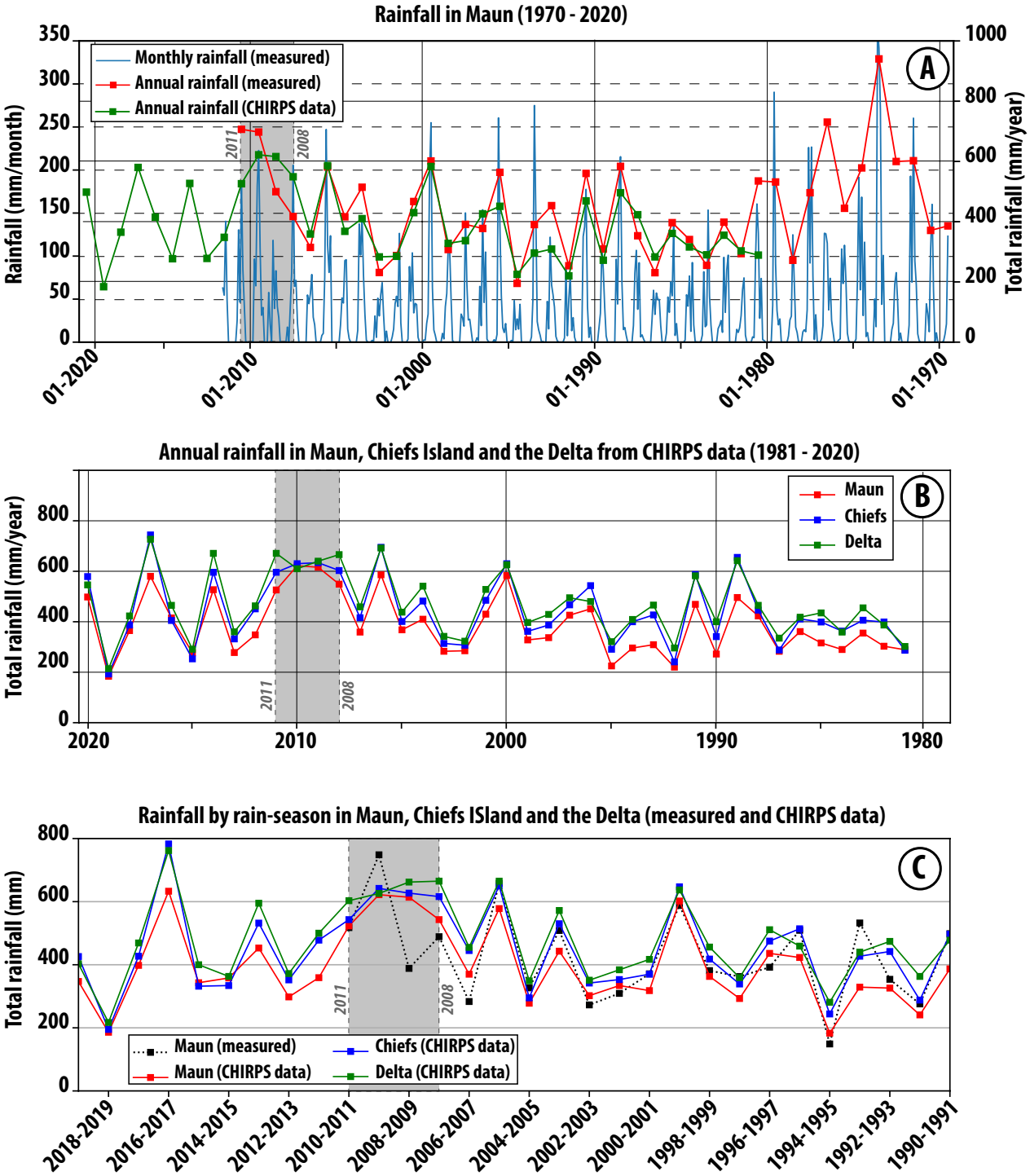

Fig. 9 **A** Rainfalls measured at Maun airport from 1970 to 2012. The blue curve corresponds to the monthly values while the red dots are total annual rainfalls. The green data are the CHIRPS annual rainfalls for the Maun pixel from 1981 to 2020. **B** CHIRPS annual rainfalls at Maun (red), in the Chiefs Island area (blue) and for the whole Delta area (green) from 1981 to 2020. **C** Total rainfall by rain-season calculated from the measured data in Maun and the CHIRPS data in Maun, Chiefs Island and the whole Delta (from season 1990–1991 to season 2019–2020). See text for discussion

probably acacias and *C. Megalobotris* (based on comparison with the present-day vegetation and the rounded, coalescent shape of the vegetation observed on the images).

In 2016, the decrease in the number of trees was 77% compared to 2006, with a total of 1627 trees. Most cell densities were down to less than 10 trees per cc except on the

Table 2 Total number of trees counted in the three zones for each year

Sheet1

	ZONE 1		ZONE 2		ZONE 3	
Years	Number	% loss	Number	% loss	Number	% loss
2018	2649	63				
2016	1627	77	286	90	361	73
2012	2293	68				
2011	3064	57				
2006	7166	0	2781	0	1338	0

%loss indicates the percentage of trees loss compared to 2006. Note that the highest value of %loss is reached in Zone-2 possibly because the considered area does not include parts of the riverine forest

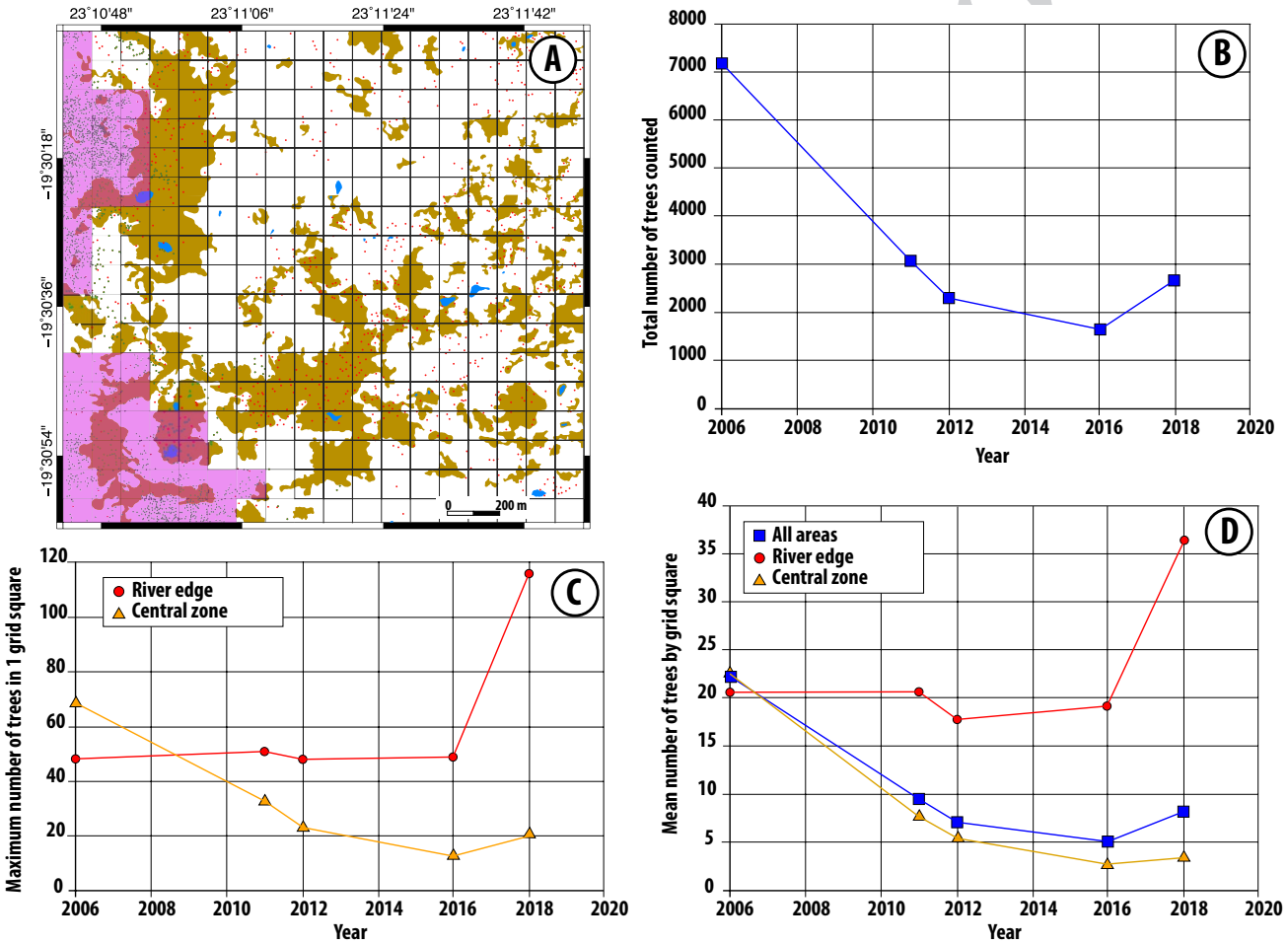

Fig. 10 Analysis of the evolution of the number of trees in Zone-1. **A** Physiographic map of Fig. 5, showing in pink the grid cells considered as the riverine forest separating the island from the floodplain. The brown areas indicate the regions corresponding to slight depressions without bushes. The blue areas are the pools containing water in 2018. **B** Evolution of the total number of trees counted in Zone-1. Note the major drop between 2006 and 2011 as well as the increase in 2018 corresponding to the expansion of the riverine forest. **C** Comparison between the number of trees in the riverine (orange) and central (red) areas. The number of trees in the riverine area is constant from 2006 to 2016 and increases sharply in 2018 with the renewed development of new species along the edges of the island. **D** Mean number of trees by grid square showing the strong influence of the riverine forest

Journal : Large 13157 | Article No : 1804 | Pages : 20 | MS Code : 1804 | Dispatch : 16-4-2024

western outer ring were the maximum remained between 45 and 50 trees per cc, increasing in the SW corner of Zone 1, the small acacia and *C. Megalobotris* bushes taking over from large trees (Fig. 6).

In 2018, most of the large trees inside the island were dead, with tree densities mostly comprised between 0 and 5 per cc. However, the total number of counted trees increased to 2649 (loss of 63% compared to 2006), for the density in the western outer ring seemed to increase rapidly, reaching a maximum of 116 trees per cc (Figs. 6 and 10). This increase, still represented by small acacia and *C. Megalobotris* bushes, was especially strong in the NW region of Zone 1.

Zone 2

A total of 2781 trees were counted in Zone 2 for 2006 (Table 2 and Sup. Fig. 2). Like in Zone 1, most of the trees were situated in low sandy zones devoid of wild sage bushes, still leaving some barren zones representing paleo channels or ephemeral channels. Indeed, in April 2006, the zone was crossed by a NW–SE channel showing flooding. In March 2021, several of those channels were flooded indicating that they remain largely active (Sup. Fig. 3). Many trees were bordering the channel active in 2006, an area which, in general corresponded to the highest density cells (up to 50 trees per cc). Zone 2 only touches the outer tree ring separating it from the Mboroga River floodplain to the east. Like in Zone 1, fallen tree trunks were visible on the ground.

In 2016, only 286 trees were counted, representing a 90% loss compared to 2006. Most cells had a tree density below 5 trees per cc except for one cell corresponding to the outer ring that displayed a density of 25 to 30 trees per cc. Like in Zone 1, those were mostly represented by small bushes, probably again of acacia and *C. Megalobotris*. The channel flooded in April 2006 was not active in February 2016 and available satellite images only show the occurrence of water in its northern part in April 2018.

Zone 3

In Zone 3, the trees were again clearly aligned along the edge of paleo-channels or in low sandy areas devoid of bushes. In 2006, 1338 trees were counted for a maximum density of 55 to 60 trees per cc in a low area corresponding to a paleo-channel (Table 2 and Sup. Fig. 2). Again, some fallen tree trunks are visible on the ground, in a number similar to that in the two other zones.

In 2016, only 361 trees were remaining (a loss of 73% compared to 2006), with a maximum density of 15 to 20 trees per cc and most of the cells containing less than 10 trees. Most of the surviving trees were still lining the paleo-channels and small bushes, probably of acacia and *C. Megalobotris* started to grow in the NE corner of the area, the closest to the outer tree ring bordering the Mboroga River floodplain.

Soil Structure, Mineral Composition and Geochemistry

The upper 40 cm of DH-1 were composed of fine-grained dark-grey sand indicating the occurrence of OM (Fig. 7). Although no rainfall was recorded during fieldwork or during the previous few days, the sediment was wet on the surface. Between 40 and 70 cm, the sediment was darker and more cohesive indicating an increase in OM and clay. From 70 to 160 cm, the color of the fine-grained sand lightened progressively and the cohesiveness decreased indicating a decrease in OM and clay content. At around 130 cm and 150 cm a series of small (around 0.5 cm in diameter) carbonated nodules (reacting to HCl) were observed. From 160 to 330 cm the fine-grained sand was pale-yellow to white, well sorted, dry and showing no obvious evidence of OM or clay. A few carbonated nodules were observed at 190 cm (0.2 cm in diameter) as well as few centimeter-large "soft pebbles" of cohesive clay-rich sand at 260 cm.

Although the surface soil around DH-2 seemed richer in clay and OM than around DH-1, only the first 20 to 25 cm of the profile showed grey to light-grey, cohesive fine-grained sand suggesting a limited amount of OM and some clay (Fig. 7). Soil humidity occurring on the surface decreased rapidly within the first 50 cm. From 25 to 160 cm the sediment was composed of fine-grained, well sorted white sand devoid of OM or clay. However, from 160 to 220 cm the amount of clay increased again, first represented by small brown "soft pebbles" then forming a cohesive and homogeneous sand-clay mixture. Humidity increased with the increase in clay content. From 220 cm, the amount of clay decreased to disappear completely around about 300 cm, the sediment corresponding again to a white, well sorted fine-grained sand. Humidity remained constantly high. From 410 to 430 cm, clay was again present in small quantity, the sand being light-brown and more cohesive. From 430 to 630 cm, the sand was white, well-sorted and the grain size increased to coarse-grained. Living roots were present with evidence of small oxidation traces (the sand was orange) probably linked to their biological activity. Finally, between 630 and 700 cm the grain size decreased again to fine-grained sand. Roots were still present and humidity was high (the drilling had to be stopped because the sand was saturated with water making it impossible to recover using the auger). This water logged sediment marks the groundwater table which we consider to be at a maximum depth given the drilling period at the end of flood season and beginning of the rain season.

The sediment composition and architecture of DH-3 contrasted with that of the two others. From 0 to 100 cm, the fine-grained sand was dark-brown, very rich in clay

Journal : Large 13157 | Article No : 1804 | Pages : 20 | MS Code : 1804 | Dispatch : 16-4-2024

(high cohesion) and rich in OM. Humidity appeared around 30 cm, increasing downward. From 100 to 170 cm, the color changed to lighter brown as OM decreased, the amount of clay still increasing. Humidity was still present. From 170 to 380 cm, small carbonated nodules (0.1 to 0.5 cm) were observed either dispersed within the clay-rich sandy matrix or concentrated on small centimeter to pluri-centimeter thick layers. Yellowish layers may have indicated the occurrence of oxides. Organic matter remained low to absent. From 390 to 430 cm, the grain size increased up to medium-grained sandstone. The OM content remained low except for some few-centimeters thick layers containing "pebbles" of OM-rich sand. Carbonated nodules were still present and a layer of small, poorly rounded gravels (0.5 cm in diameter) was observed at 420 cm. From 420 to 530 cm, the sand was again fine-grained still containing a high amount of clay but fewer carbonated nodules. The latests tended to be smaller and more elongated than those in the upper part of the log. Oxidation levels were visible, probably corresponding to present-day root activity as suggested by the presence of root fragments in the samples. The depth of 530 cm marked a very sharp transition to white, very well sorted fine-grained sand completely devoid of clay, OM or nodules. The log was stopped at 600 cm, still in that white sand.

The geochemical composition of samples from DH-1 and DH-2 reflects the differences observed in the soil structure and first-order petrographic analysis (Table 1). In general, the samples are largely dominated by SiO_2 with only a limited amount of CaO (maximum value of 2.88%) that matches the presence of few pedogenic carbonate nodules. Na_2O and K_2O values are also low (less than 0.03% and 0.3% respectively) excluding the presence of salt even on the surface. The K_2O, associated to the low Al_2O_3 content (less than 2.3%) indicate the presence of clay, the highest values being correlated with the highest LOI (loss on ignition) values that correspond both to the de-hydration of clay and the burning of OM.

In samples from DH-1, CaO concentration increases slightly from 150 cm, reaching a maximum of 2.9% at 194 cm. This variation matches the occurrence of carbonates nodules from 130 cm as well as the well-identified nodules at 190 cm. This depth probably corresponds to the lower limit of strong root activity, allowing for the carbonates to precipitate. Jolivet et al. (2023) also indicated, from drillings in Nxaraga Island, immediately west of the drilling sites on Chiefs Island, that the first appearance of carbonate nodules corresponds to the maximum level of the ground water table. Samples below 194 cm also display a marked decrease in K_2O and AL_2O_3 content and in LOI values. This is consistent with the observed decrease in clay and OM content below 160 cm. The simultaneous decrease in Fe_2O_3 and TiO_2 may corresponds to a decrease in the amount of Fe-Ti oxides generally associated to OM.

In samples from DH-2 most concentrations are low which matches the observed absence of pedogenic carbonates as well as the limited amount of clay and OM (LOI < 1% except on the surface). The absence of pedogenic carbonates suggests that root activity encompasses the whole lengths of the profile. This is further supported by the occurrence of leaving roots down to the base of the profile.

Flood and Rainfall Analysis

The annual flood that irrigates the Okavango alluvial fan has been monitored at Mohembo station since 1933 and studied for several decades (McCarthy et al. 2000; Milzow et al. 2009; Dauteuil et al. 2023). At the station, the high flood occurs between April and May, while the low flood period extends from October to November. Further south at the latitude of Chiefs Island, these periods are shifted towards July – August and December – January, respectively. The flood intensity is multi-cyclic. A main cycle at 48 years for the average annual flow is accompanied by a 17.5 years cycle and a 7.8 years cycle both in the annual average and maximum flows (McCarthy et al. 2000; Mazvimavi and Wolski 2006). These cycles are related to several parameters including tropical multi-decadal oscillations, water circulation and temperature changes in the Atlantic (such as the El Niña current) and changes in temperature contrast between the continent and Indian Ocean (Jury 2013).

Data from December 1974 to May 2022 compiled on Fig. 7 show that following a high flood regime in the 1970th, a low regime was installed during the 1980th – 1990th, reaching its minimum between 1993 and 1998. From then on, the flood intensity increased again, reaching a maximum during the period 2009 – 2012, with a peak value in the Okavango River discharge of more than 1100 m^3/s in 2010 (Fig. 8), before declining again. The overall minimum flood peak (maximum discharge just above 200 m^3/s) was reached in 2019, the flood not reaching the toe of the Delta near Maun that year.

As shown on Fig. 9A, the annual precipitation values measured at Maun airport are generally consistent with those provided by the CHIRPS data for the pixel corresponding to Maun. However some non-negligible discrepancies occur, especially in the years 1992–1993 and 2008–2011. We have no constrains on the accuracy of the measurements made at Maun airport and cannot determine the reasons for the observed differences between the two datasets. The on-site measurements might be more sensible to local rainfall during thunder-storms than the CHIRPS data that integrate daily rainfalls with a resolution of 0.05° (c.a. 5 × 5 km pixel). Alternatively, the CHIRPS data assimilate ground station data and the discrepancy between the two records might correspond to periods when the Maun data were not provided to the CHIRPS program. Figure 9B is a comparison between

Journal : Large 13157 | Article No : 1804 | Pages : 20 | MS Code : 1804 | Dispatch : 16-4-2024

the annual rainfall at Maun, the Chiefs Island area and the overall Delta (see Fig. 1). The values at Maun are generally slightly lower than in the two other zones which have very similar annual rainfalls.

Similarly to the flood, annual rainfalls in the Okavango Delta are also variable with a peak value of 940 mm measured at Maun airport in 1974 and a lowest value of c.a. 200 mm either measured or calculated from CHIRPS in 1992, 1995, and 2019. However, a cyclic signal in those data is less obvious than in the flood regime. It has been suggested from measured data ranging from 1961 to 2003 that rainfall had increased until 1981 before decreasing until 2003 (Parida and Moalafhi 2008). Large values have been reached later, especially in 2010 (697 mm) and 2011 (706 mm) (Fig. 9A) but these measurements have to be taken with caution as the CHIRPS data indicate values of 622 and 526 mm respectively. What is noticeable however is the period 2008–2010. Annual rainfalls of 600 mm or more are generally peak values, lasting only one year before decreasing significantly the next year. Between 2008 and 2010, annual rainfalls remained around or above 600 mm in Chiefs Island and the Delta, while slightly lower at Maun in 2008 and 2011.

Instead of considering calendar years, we calculated the total rainfall for each rain seasons (Fig. 9C). While most values fall between 300 and 500 mm/yr, the period 2008 – 2010 is again characterized by values above 600 mm in the Delta and Chiefs Island. The value in the Delta remained at 600 mm during the season 2010–2011 while in Chiefs Island, the value slightly decreased to 540 mm. The period 2008–2011 thus represents the wettest period recorded since the mid-1970th.

Discussion

The death of between 70 and 80% of the trees in the southern part of Chiefs Island between 2006 and 2016, with 50 to 60% of mortality between 2006 and 2011 reflects a major shift in the savanna woodland type ecosystem characterizing the largest island of the Okavango Delta (Table 2). Furthermore, it is to be noted that no high-resolution satellite images are available between 2006 and 2011, preventing a more detailed analysis of the timing. The mortality measured in this study might thus have been reached before 2011, implying very high mortality rates. Finally, the riverine woodland vegetation forming the outer ring of the island was affected differently by the major stress event that killed the trees inside the island. Indeed, the tree density data indicate that this area, after loosing its large trees between 2011 and 2012 mainly continued its development, with a noticeable increase in the number of trees from 2016 to 2018 (Fig. 10). Vegetation in that area separating the Boro floodplain from Chiefs Island is more diversified, with a high proportion of *C. Megalobotris* that commonly grow on floodplain margins and in riverine forests (Heath and Heath 2009).

Several mechanisms that could explain the catastrophic evolution of the forest cover inside Chiefs Island can be excluded:

- No evidence of bush fire were observed on the fallen trees and the extension of the Dead Forest would have required major fires. Figure 11 shows the yearly extend of bush fire in the area of Chiefs Island between 2006 and 2020, based on remote sensing MODIS data (Giglio et al. 2015). Although major fires affect the Okavango Delta every year, Chiefs Island is relatively preserved and only small areas have burned in 2012, 2013 and 2015. None of the selected study areas have been affected by those fires which correlates with the absence of field evidence. Furthermore, locally trees have been dying through several years which is incompatible with destruction by fire. Finally, both *C. mopane* and acacias have a similar medium tolerance to fire (Barnes 2001; Burke 2006) which would not explain why the formers seem to have partly survived the major stress event while acacias did not.
- Although the soil samples have been collected some 10 to 15 years after the death of the trees, chemical poisoning by salt deposited on the surface can be reasonably rejected. The geochemical data obtained on soil profiles in Zone 1 exclude the occurrence of salt, either on the surface or at depth down to 7 m. While dissolution and rinsing by rain water may be expected on the near surface, a salt concentration lethal to the relatively salt-tolerant *C. mopane* (Makhado et al. 2014) should still be detectable at depth. Furthermore, reaching such a concentration on the surface would need either the rise of highly alkaline ground water such as the one observed on several other islands (Ellery and McCarthy 1994; Bauer et al. 2004; Ramberg and Wolski 2008; Dauteuil et al. 2021), or a massive dissolution – precipitation event. In both cases traces of that salt should be found in the deep sediment (Jolivet et al. 2023, 2024).
- No major drought event occurred during the observation period, the annual rainfall values and flood discharge being equal or higher than during the previous decades. Furthermore, *C. mopane* and acacias that represent most of the savanna woodland species are resistant to drought (Barnes et al. 1997; Barnes 2001; Makhado et al. 2014; Krug 2017).

While extreme or extra-seasonal drought events are generally seen as major drivers for forest dieback in semi-arid climates, exceptional soil water logging and flooding can also lead to major tree death (White 2007; Parolin and

Journal : Large 13157 | Article No : 1804 | Pages : 20 | MS Code : 1804 | Dispatch : 16-4-2024

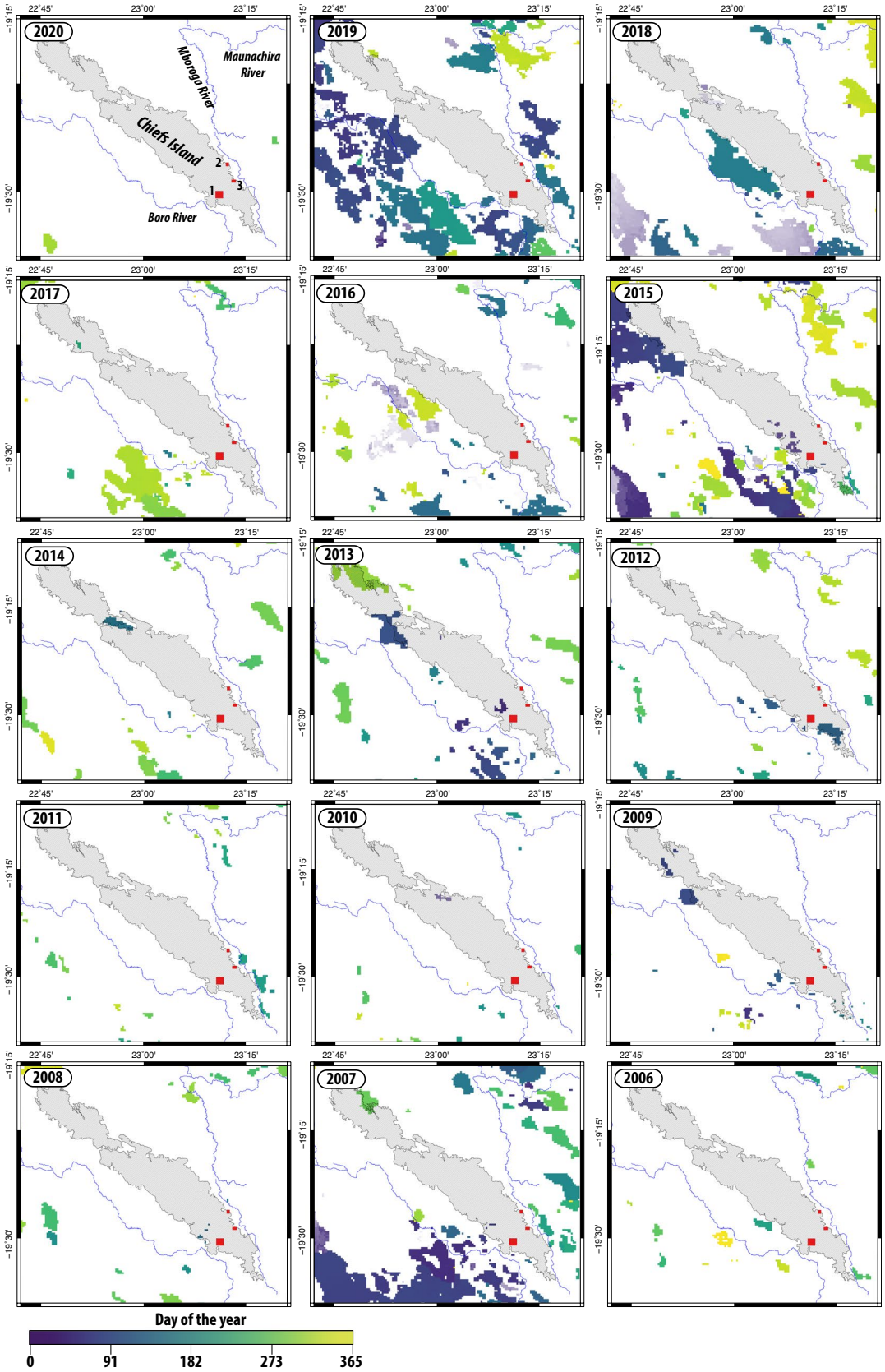

Journal : Large 13157 | Article No : 1804 | Pages : 20 | MS Code : 1804 | Dispatch : 16-4-2024

◂**Fig. 11** Maps of the yearly burned areas in the vicinity of Chiefs Island from 2006 to 2020. The maps were compiled using the MODIS monthly Burned Area product, with a spatial resolution of 500 m (Giglio et al. 2015). The colors correspond to the day of the year surfaces were burnt. The red rectangles indicate the position of the three zones used for tree counting. Note that, based on those data, the 3 counting areas were not affected by fire during the considered period

Wittmann 2010; Basak et al. 2015). Dieback of woody species as been observed in the distal region of the Delta where channels that had remained dry for several decades and had been colonized by *acacia tortillis* woodlands, were suddenly flooded in 2008/2009 and 2009/2010 (Wolski et al. 2012). High resolution satellite images available on Google Earth show that Chiefs Island is not the only place were large-scale tree dieback occurred between 2006 and 2018. Supplementary Fig. 4 shows the evolution of the forest along the southern banks of the Maunachira River near the locality of Kwaï (Fig. 1) from 2006 to 2018. The 2006 image shows a high density of trees bordering the river but during the major flood event of 2010, a large area of the forest was flooded, the water being still present in December 2010 (the date of the picture). Flooding of that area probably also occurred during the major flood of 2011 as the image taken in April 2012 still shows large pools in the previously inundated zone. From Fig. 7, the 2009 flood was nearly as high as 2011 which suggest that the banks of the Maunachira River might also have been flooded. In December 2010, most of the trees in the flooded area were still standing, although most of them were leafless. In April 2012, all the trees affected by flooding – but a few exceptions – were still leafless (while those outside the flooded area had leafs) and many logs had fallen on the ground. The August 2018 image clearly shows that all the trees in the area flooded in 2010 and most probably in 2009 and 2011 were dead, which we confirmed during field work in July 2022. The dieback encompasses areas situated immediately around the flood zone most probably showing the extend of major soil water logging. Similarly, Supplementary Fig. 5 shows the vegetation around a pool situated in the central part of a large island immediately south of Chiefs Island (Fig. 3), from 2006 to 2020. The November 2006 image has a relatively low resolution but numerous trees are clearly visible around the pool. The next image, taken in July 2011 shows that many of the trees were dead, some logs already fallen on the ground. However, some large trees had survived in the immediate vicinity of the pool. In May 2012, only a few trees were alive along the southern edge of the pool, while in June 2020, all of them were dead.

Based on these observations and the data described above, we suggest that the exceptional floods of 2009, 2010 and 2011, associated to the constantly heavy rainfalls during the 2008 to 2011 rain seasons generated unusual hydrological conditions with large inundated areas and/or long-term water logged soil. These extreme environmental conditions caused the major tree dieback on Chiefs Island and in the surrounding areas. Except for the sandy ridge of DH-1, the soil of Chiefs Island that we investigated revealed a high humidity content during the dry season (July 2022) or at the very beginning of the rain season (November 2021). A number of pools, including the one near DH-3 show surface water on most available satellite images. Drill hole DH-2 had to be stopped at 7 m depth when reaching water saturation providing indication on the water table level at the end of the flood season and before the rain season. The flood in 2021 was very limited (peak discharge at about 300 m^3/s at Mohembo station) compared to the floods in 2009 – 2012 (peak discharge at about 1100 m^3/s in 2010) (Fig. 8). However, the satellite image of March 2021 still shows a large number of inundated channels on Zone 2, indicating that water logging may occur even during those low-flood years (Sup. Fig. 3). As shown above, the 2009 – 2012 high floods were associated to high rainfall values (Fig. 9C). We suggest that the combination over 3 to 4 consecutive years of high flood leading to high underground water recharge during the flood season (May to September), and heavy rain leading to water saturation of the surface sediment during the rainy season (October to March), induced a prolonged water logging (at least for 3 years without the usual water-table lowering and surface drying linked to the flood receding) that was lethal to the large trees. While acacias, and especially *Acacia erioloba* have deep tap roots (Barnes et al. 1997; Barnes 2001), *C. mopane* is a shallow-rooted species, with most of the roots between 20 and 120 cm from the surface (Smit and Rethman 1998). Both tree species are well adapted to drought. Acacias will favor deep sandy soil, using their deep tap root to pump ground water during the dry season. *C. mopane* will favor clay-rich, alkaline, poorly drained soils, relying on its important shallow roots density to absorb rain water and adapting its physiology during the driest season mostly by loosing its leaves (Makhado et al. 2014). However, if those trees are adapted to drought, they cannot sustain prolonged periods of inundation as shown by the examples described above along the Maunachira River. The ability of flooding to kill large trees through root rotting and respiration impeding has been long demonstrated (Davidson 1997; White 2007; Basak et al. 2015), and Basak et al. (2015) noted that the oldest trees are the most affected.

C. mopane is highly competitive and may survive short periods of water logging (Krug 2017), which might explain why some of the large mopane trees survived the prolonged period of recurrent inundation from 2009 to 2012. Furthermore, since this is a shallow rooted species, the trees might have benefited from a limited decrease in surface water logging during the dry season. Acacias, with their deeper tap roots did not have that opportunity, the groundwater level remaining high from flood and rain recharge. Finally,

the different vegetation in the western outer ring of Chiefs Island, more adapted to riverine environments (as *C. Megalobotris* for example) were less affected by the long-lasting water logging conditions. While large acacia, mopanes or lead wood trees growing in that area were killed, the other species survived and started expanding toward the newly created opened environment inside the island (Fig. 6).

The large-scale drowning event that affected the southern part of Chiefs Island in 2009 – 2012 most probably had a profound impact on the local ecosystem that remains to be documented. The destruction of the initial savanna forest induced a high degree of selection within the tree species. Acacias having disappeared from the central part of the island, *C. mopane* is now taking over, making for a less diverse flora. This in turn may have some implications on the ecosystem: while *C. mopane* leaves are nutritious and thus preferentially browsed by large herbivores (Makhado et al. 2018), the loss of tree biodiversity may have an impact on both the smaller fauna, the flora and the underground micro-ecosystems. Finally, the loss of tree cover should favor soil erosion (especially aeolian transport of sand) and increase the ground temperatures, which in turn should increase potential evapotranspiration (Wolski 2009) enhancing the local effects of global warming. Nonetheless, the potential effects of climate warming on the hydrology of the Okavango are still difficult to assess, maintaining uncertainties on the ecological future of this hot-spot of biodiversity. Based on a combination of satellite, meteorological and river flow data, Jury (2013) demonstrated that in Africa the period 1995 – 2010 has been noticeably wet compared to the previous decades (as far as the 1950s), culminating in the major rainfall and flood events of 2008—2010. In the Zambezi system, the author relates the three folds increase in rainfall observed between 1995 and 2010 to a stronger land-sea temperature contrast (continental air temperature, especially in the Kalahari increased) bringing more humid air from the Indian ocean towards equatorial Africa and the upper Zambezi drainage area. This large-scale model thus suggest that an increase in continental air temperature should result in larger rainfall and flood events. Oppositely, Wolski et al. (2014) using a global atmospheric model coupled to a hydrological model, concluded that anthropogenic emissions in the atmosphere indeed increase the temperatures but generally decrease rainfall over the Okavango drainage system, limiting the intensity of the floods. Furthermore, higher temperatures should strengthen potential evapotranspiration which in turn will allow the permeable sandy soil of the Okavango alluvial fan to dry faster, lowering the groundwater table and thus limiting the propagation of the next flood (Gumbricht et al. 2004; Milzow et al. 2009; Wolski et al. 2014). Following that model, global warming should reduce the probability of high floods. Although this would probably affect the ecology of the Delta, it should reduce the forest drowning effect described above, limiting soil denudation.

Conclusion

While most ecological studies looking at the effects of climate change in semi-arid savannas are investigating the impact of increased temperature and drought conditions, we advocate that drowning events should also be considered as a major driver for the ecosystem dynamics. The Okavango Delta wetlands represent a highly valuable hot-spot of biodiversity within the Kalahari desert. This ecosystem will certainly be affected by global warming but its internal complexity combined to the uncertainties in climate forecasting models, make it difficult to distinguish between natural evolution and induced changes. Indeed, the impact of regional climate change might be masked behind natural variations in flood and rain intensity, river avulsion mechanisms, surface changes due to tectonic activity or autocyclic flora and fauna dynamics. Is the rapid and massive death of southern Chiefs Island's forest an autocyclic mechanism or allocyclic mechanism remains to be assessed. In any case, preservation efforts in the Okavango Delta will require transdisciplinary studies of its ecosystem and an increased effort in field monitoring of both biological, climatic and geological indicators.

Supplementary Information The online version contains supplementary material available at https://doi.org/10.1007/s13157-024-01804-9.

Acknowledgements This work was supported by the CNRS-MITI International Emerging Projects program and the CNRS-INSU Tellus program. We are grateful to the Government of Botswana and the Ministry of Environment, Natural Resources conservation and Tourism for delivering us a research permit (permit number ENT 8/36/4L (83)) and access to the Moremi Game Reserve. The Okavango Research Institute provided complete field logistic and valuable technical and scientific advises. Two anonymous reviewers, the Associate Editor and Editor in Chief M.L. Otte have promoted an interesting discussion that greatly improved the manuscript.

Authors Contributions Marc Jolivet designed the study, collected the remote-sensing and field data and wrote the manuscript. Mike Murray Hudson participated in the analysis of the data and provided insight during the discussion. Kaelo Makati, Olivier Dauteuil and Louis Gaudaré participated in collecting the field data and in the analysis of the results.

Funding This work was supported by the CNRS-MITI International Emerging Projects program and the CNRS-INSU Tellus program. No grant numbers are attached to these fundings.

Data Availability The dataset generated and analyzed during the current study are available from the corresponding author on reasonable request.

Declarations

Competing Interest The authors have no relevant financial or non-financial interests to disclose.

References

Barnes ME (2001) Effects of large herbivores and fire on the regeneration of *Acacia erioloba* woodlands in Chobe National Park, Botswana. African Journal of Ecology 39:340–350

Barnes RD, Fagg CW, Milton SJ (1997) *Acacia erioloba*. Tropical Forestry Papers, 35, Nuffield Press, Oxford, UK, 66p. ISBN:0 85074 143 2

Basak SR, Basak AC, Ataur Rahman M (2015) Impacts of floods on forest trees and their coping strategies in Bangladesh. Weather and Climate Extremes 7:43–48

Bauer P, Thabeng G, Stauffer F, Kinzelbach W (2004) Estimation of the evapotranspiration rate from diurnal groundwater level fluctuations in the Okavango Delta, Botswana. Journal of Hydrology 288(3):344–355. https://doi.org/10.1016/j.jhydrol.2003.10.011

AQ11 Bauer P, Gumbricht T, Kinzelbach W (2006) A regional coupled surface water/groundwater model of the Okavango Delta, Botswana. Water Resources Research 42:W04403. https://doi.org/10.1029/2005WR004234

Biggs RC (1979) The ecology of Chief's Island and the adjacent floodplains of the Okavango Delta, Botswana. MsC Dissertation, Faculty of Science, University or Pretoria, Pretoria, South Africa, 315p

Burke A (2006) Savanna trees in Namibia – Factors controlling their distribution at the arid end of the spectrum. Flora 201:189–201

Bush ER, Whytock RC, Bahaa-el-din L, Bourgeois S, Bunnefeld N et al (2020) Long-term collapse in fruit availability threatens Central African forest megafauna. Science 370(6521):1219–1222

Christensen JH, Hewitson B, Busuioc A, Chen A, Gao X, Held I, Jones R, Kolli RK, Kwon W-T, Laprise R, Magana Rueda V, Mearns L, Menendez CG, Raisanen J, Rinke A, Sarr A, Whetton P (2007) Regional climate projections. In: Qin SD, Manning M, Chen Z, Marquis M, Averyt KB, Tignor M, Miller HL (eds) Climate change 2007: the physical science basis. Contribution of working group I to the fourth assessment report of the intergovernmental panel on climate change Solomon. Cambridge University Press, Cambridge

AQ12

Cunningham PL, Detering F (2017) Determining age, growth rate and regrowth for a few tree species causing bush thickening in north-central Namibia. Namibian Journal of Environment 1:72–76

Dauteuil O, Jolivet M, Dia A, Murray-Hudson M, Makati K, Barrier L, Bouhnik Le Coz M, Audran A, Radenac A (2021) Trace metal enrichments in water of the Okavango Delta (Botswana): hydrological consequences. Geochemistry, Geophysics, Geosystems 22:e2021GC009856. https://doi.org/10.1029/2021GC009856

Dauteuil O, Jolivet M, Gaudaré L, Pastier A-W (2023) Rainfall-induced ground deformation in southern Africa. Terra Nova. https://doi.org/10.1111/ter.12650

Davidson EM (1997) Are jarrah (*Eucalyptus marginata*) trees killed by *Phytophthora cinnamoni* or waterlogging? Australian Forestry 60:116–124

Ellery WN, McCarthy TS (1994) Principles of sustainable utilization of the Okavango Delta ecosystem, Botswana. Biological Conservation 70:159–168

Funk CC, Peterson P, Landsfeld M, Pedreros D, Verdin J, Shukla S, Husak G, Rowland J, Harrison L, Hoell A, Michaelsen J (2015) The climate hazards infrared precipitation with stations – a new environmental record for monitoring extremes. Scientific Data 2:150066. https://doi.org/10.1038/sdata.2015.66

Funk CC, Peterson PJ, Landsfeld MF, Pedreros DH, Verdin JP, Rowland JD, Romero BE, Husak GJ, Michaelsen JC, Verdin AP (2014) A quasi-global precipitation time series for drought monitoring. U.S. Geological Survey Data Series 832, 4p. https://doi.org/10.3133/ds832

Giglio L, Justice C, Boschetti L, Roy D (2015) *MCD64A1 MODIS/Terra+Aqua Burned Area Monthly L3 Global 500m SIN Grid V006* . NASA EOSDIS Land Processes Distributed Active Archive Center. Accessed 2024-01-19 from https://doi.org/10.5067/MODIS/MCD64A1.006

Gumbricht T, McCarthy TS, Merry CL (2001) The topography of the Okavango Delta, Botswana, and its tectonic and sedimentological implications. South African Journal of Geology 104:243–264

Gumbricht T, Wolski P, Frostc P, McCarthy TS (2004) Forecasting the spatial extent of the annual flood in the Okavango delta, Botswana. Journal of Hydrology 290:178–191

Hansen MC, Potapov PV, Pickens AH, Tyukavina A, Hernandez-Serna A, Zalles V, Turubanova S, Kommareddy I, Stehman SV, Song X-P, Kommareddy A (2022) Global land use extent and dispersion within natural land cover using Landsat data. Environmental Research Letters 17:034050. https://doi.org/10.1088/1748-9326/ac46ec

Hartmann H, Bastos A, Das AJ, Esquivel-Muelbert A, Hammond WM, Martínez-Vilalta J, McDowell NG, Powers JS, Pugh TAM, Ruthrof KX, Allen CD (2022) Climate change risks to global forest health: emergence of unexpected events of elevated tree mortality worldwide. Annual Reviews of Plant Biology 73:673–702

Heath A, Heath R (2009) Field guide to the plants of Northern Botswana including the Okavango Delta. Goyder D (ed) Kew Publishing, Royal Botanic Gardens, Kew, UK. ISBN: 978–1–84246–183–9

IPCC (2002) Climate change 2022: impacts, adaptation, and vulnerability. contribution of working group II to the sixth assessment report of the intergovernmental panel on climate change [Pörtner H-O, Roberts DC, Tignor M, Poloczanska ES, Mintenbeck K, Alegría A, Craig M, Langsdorf S, Löschke S, Möller V, Okem A, Rama B (eds)]. Cambridge University Press. Cambridge University Press, Cambridge, 3056 pp. https://doi.org/10.1017/9781009325844

Jolivet M, Dauteuil O, Dia A, Davranche M, Pierson-Wickmann AC, Barrier L, Murray-Hudson M, Mazrui N, Cheng F, Li X (2023) Highly contrasted geochemical pattern in sediment of the Okavango Delta, Botswana driven by dust supply, hydrological heritage and biogeochemical reactions. Geochemistry, Geophysics, Geosystems 24:e2023GC010978. https://doi.org/10.1029/2023GC010978

Jolivet M, Dauteuil O, Dia A, Davranche M, Pierson-Wickmann AC, Barrier L, Murray-Hudson M, Mazrui N, Cheng F, Li X (2024) Reply to comment by Terence McCarthy and Marc Humphries on "highly contrasted geochemical pattern in sediments of the Okavango Delta, Botswana driven by dust supply, hydrological heritage and biogeochemical reactions." Geochemistry, Geophysics, Geosystems 25:e2023GC011315. https://doi.org/10.1029/2023GC011315

Jump AS, Ruiz-Benito P, Greenwood S, Allen CD, Kitzberger T, Fensham R, Martinez-Vilalta J, Lloret F (2017) Structural overshoot of tree growth with climate variability and the global spectrum of drought)induced forest dieback. Global Change Biology 23(9):3742–3757

Jury M (2013) A return to wet conditions over Africa: 1995–2010. Theoretical and Applied Climatology 111(3–4):471–481

Kenabatho PK, Parida BP, Moalafhi DB (2012) The value of large-scale climate variables in climate change assessment: the case of Botswana's rainfall. Physics and Chemistry of the Earth 50–52:64–71

Krug JHA (2017) Adaptation of Colophospernum mopane to extra-seasonal drough conditions: site-vegetation relations in dry-deciduous forests of Zmabezi region (Namibia). Forest Ecosystems 4:25. https://doi.org/10.1186/s40663-017-0112-0

Makhado RA, Mapaure I, Potgieter MJ, Luus-Powell WJ, Saidi AT (2014) Factors influencing the adaptation and distribution of *Colophospernum mopane* in southern Africa's mopane savanna – a review. Bothalia 44(1):1–9 (art. #152)

Makhado RA, Potgieter MJ, Luus-Powell WJ (2018) Colophospernum mopane leaf production and phenology in Southern

Africa's savanna ecosystem – a review. Insights of Forest Research 2(1):84–90
Masike S, Urisch P (2008) Vulnerability of traditional beef sector to drought and the challenges of climate change: the case of Kgatleng District, Botswana. Journal of Geography and Regional Planning 1:012–018
Mazvimavi D, Wolski P (2006) Long-term variations of annual flows of the Okavango and Zambezi Rivers. Physics and Chemistry of the Earth 31:944–951
McCarthy TS (2013) The Okavango Delta and its place in the geomorphological evolution of Southern Africa. South African Journal of Geology 116(1):1–54. https://doi.org/10.2113/gssajg.116.1.1
McCarthy TS, Ellery WN (1994) The effect of vegetation on soil and ground water chemistry and hydrology of islands in the seasonal swamps of the Okavango Fan, Botswana. Journal of Hydrology 154:169–193
McCarthy TS, McIver JR, Cairncross B (1986) Carbonate accumulation on islands in the Okavango Delta, Botswana. South African Journal of Science 82:588–591
McCarthy TS, McIver JR, Verhagen BTh (1991) Groundwater evolution, chemical sedimentation and carbonate brine formation on an island in the Okavango Delta swamp, Botswana. Applied Geochemistry 6:577–595
McCarthy TS, Barry M, Bloem A, Ellery WN, Heister H, Merry CL, Rüther H, Sternberg H (1997) The gradient of the Okavango fan, Botswana, and its sedimentological and tectonic implications. Journal of African Earth Sciences 24:65–78
McCarthy TS, Cooper GJR, Tyson PD, Ellery WN (2000) Seasonal flooding in the Okavango Delta - recent history and future prospects. South African Journal of Science 96:25–33
McGregor SD, O'Connor TG (2002) Patch dieback of *Colophospernum mopane* in a dysfunctional semi-arid African savanna. Austral Ecology 27:385–395
Mendelsohn J, VanderPost C, Ramberg L, Murray-Hudson M, Wolski P, Mosepele K (2010) Okavango Delta: floods of life. RAISON (Windhoek, Namibia). ISBN: 978–99916–780–5–4
Milzow C, Kgotlhang L, Bauer-Gottwein P, Meier P, Kinzelbach W (2009) Regional review: the hydrology of the Okavango Delta, Botswana—processes, data and modelling. Hydrogeology Journal 17(6):1297–1328. https://doi.org/10.1007/s10040-009-0436-0
Parida BP, Moalafhi DB (2008) Regional rainfall frequency analysis for Botswana using L-Moments and radial basis function network. Physics and Chemistry of the Earth 33:614–620
Parolin P, Wittmann F (2010) Struggle in the flood: tree responses to flooding stress in four tropical floodplain systems. AoB Plants 2010:plq003. https://doi.org/10.1093/aobpla/plq003
Pastier A-M, Dauteuil O, Murray-Hudson M, Moreau F, Walpersdorf A, Makati K (2017) Is the Okavango Delta the terminus of the East African Rift System? Towards a new geodynamic model: geodetic study and geophysical review. Tectonophysics 712–713(Supplement C):469–481. https://doi.org/10.1016/j.tecto.2017.05.035
Pietrykowski M, Woś B (2021) The impact of climate change on forest tree species dieback and changes in their distribution. In: Choudhary DK, Mishra A, Varma A (eds) Climate change and the microbiome. Soil biology, vol 63. Springer, Cham. https://doi.org/10.1007/978-3-030-76863-8_23
Ramberg L, Wolski P (2008) Growing islands and sinking solutes: processes maintaining the endorheic Okavango Delta as a freshwater system. Plant Ecology 196(2):215–231. https://doi.org/10.1007/s11258-007-9346-1
Ramberg L, Hancock P, Lindholm M, Meyer T, Ringrose S, Sliva J, Van As J, VanderPost C (2006a) Species diversity of the Okavango Delta, Botswana. Aquatic Science 68:310–337
Ramberg L, Wolski P, Krah M (2006b) Water balance and infiltration in a seasonal floodplain in the Okavango Delta, Botswana. Wetlands 26(3):677–690
Retallack GJ (2005) Pedogenic carbonate proxies for amount and seasonality of precipitation in paleosols. Geology 33(4):333–336
Roodt V (1992) The Shell field guide to common trees of the Okavango Delta and Moremi Game Reserve. Shell Oil, Botswana (Pty) Ltd, 110p
Ruosteenoja K, Carter TR, Jylha K, Tuomenvirt H (2003) Future climate in world regions: an intercomparison of model-based projections for the new IPCC emissions scenarios. Finnish Environment Institute No. 644, Helsinki. 83pp
Sebego RJG (1999) The ecology and distribution limits of *Colophospernum mopane* in southern Africa. Botswana Notes and Records 31:53–72
Smallie JJ, O'Connor TG (2000) Elephant utilization of Colophospernum mopane: possible effects of hedging. African Journal of Ecology 38:1–9
Smit GN, Rethman NFG (1998) Root biomas depth distribution and relations with leaf biomass of *Colophospernum mopane*. South African Journal of Botany 64:38–43
Vancutsen C, Achard F, Pekel J-F, Vieilledent G, Carboni S, Simonetti D, Gallego J, Aragão LEOC, Nasi R (2021) Long-term (1990–2019) monitoring of forest cover changes in the humid tropics. Science Advances 7:eabe1603
White TCR (2007) Flooded forests: death by drowning, not herbivory. Journal of Vegetation Science 18:147–148
Wolski P, Savenije HHG (2006) Dynamics of floodplain-island groundwater flow in the Okavango Delta, Botswana. Journal of Hydrology 320:283–301
Wolski P, Todd MC, Murray-Hudson MA, Tadross M (2012) Multi-decadal oscillations in the hydro-climate of the Okavango River system during the past and under a changing climate. Journal of Hydrology 475:294–305. https://doi.org/10.1016/j.jhydrol.2012.10.018
Wolski P (2009) Assessment of hydrological effects of climate change in the Okavango Basin. Okavango Basin Transboundary Diagnostic Analysis Report, OKACOM, Maun, Botswana, 67p
Xu C, McDowell NG, Fisher RA, Wei L, Sevanto S et al (2019) Increasing impacts of extreme droughts on vegetation productivity under climate change. Nature Climate Change 9(12):948–953

Journal:	**13157**
Article:	**1804**

Author Query Form

Please ensure you fill out your response to the queries raised below and return this form along with your corrections

Dear Author

During the process of typesetting your article, the following queries have arisen. Please check your typeset proof carefully against the queries listed below and mark the necessary changes either directly on the proof/online grid or in the 'Author's response' area provided below

Query	Details Required	Author's Response
AQ1	Please check if the affiliations are presented and captured correctly.	
AQ2	Please check if the article title is captured correctly.	
AQ3	Ref. "Ramberg et al. 2006, Wolski et al. 2014" are cited in the body but its bibliographic information is missing. Kindly provide its bibliographic information in the list.	
AQ4	IPCC, 2022 has been changed to IPCC, 2002 so that this citation matches the Reference List. Please confirm that this is correct.	
AQ5	Pietrzykowski and Wós, 2021 has been changed to Pietrykowski and Woś, 2021 so that this citation matches the Reference List. Please confirm that this is correct.	
AQ6	Please check if all figure captions are presented/captured correctly.	
AQ7	Vancutsem et al., 2021 has been changed to Vancutsen et al., 2021 so that this citation matches the Reference List. Please confirm that this is correct.	
AQ8	Hansen et al., 2021 has been changed to Hansen et al., 2022 so that this citation matches the Reference List. Please confirm that this is correct.	
AQ9	Tables 1 and 2 were captured as fx table, please check if captured correctly.	
AQ10	Davison, 1997 has been changed to Davidson, 1997 so that this citation matches the Reference List. Please confirm that this is correct.	
AQ11	References [Bauer et al. (2006), Christensen et al. (2007), Gumbricht et al. (2001), Kenabatho et al. (2012), Masike and Urisch (2008), McCarthy et al. (1997), Ruosteenoja et al. (2003)] were provided in the reference list; however, this was not mentioned or cited in the manuscript. As a rule, all references given in the list of references should be cited in the main body. Please provide its citation in the body text.	
AQ12	Publisher location "Cambridge" were captured in references [Christensen et al., 2007, IPCC, 2002], please check if correct.	